

1 **Title.** Physicochemical and Urban Land-Use Characteristics Associated with Resistance to  
2 Precipitation in Estuaries Vary Across Scales

3

4 **Authors and Affiliations**

5 *Anna B. Turetcaia* 0000-0003-1630-5741<sup>1,\*</sup>, [anna.turetcaia@pnnl.gov](mailto:anna.turetcaia@pnnl.gov)

6 *Nicole G. Dix* 0000-0002-0063-5167<sup>2</sup>, [nikki.dix@dep.state.fl.us](mailto:nikki.dix@dep.state.fl.us)

7 *Hannah Ramage* 0009-0004-2246-7696<sup>3</sup>, [hannah.ramage@wisc.edu](mailto:hannah.ramage@wisc.edu)

8 *Matthew C. Ferner* 0000-0002-4862-9663<sup>4</sup>, [mferner@sfsu.edu](mailto:mferner@sfsu.edu)

9 *Emily B. Graham* 0000-0002-4623-7076<sup>1,5,\*</sup>, [emily.graham@pnnl.gov](mailto:emily.graham@pnnl.gov)

10

11 <sup>1</sup> Pacific Northwest National Laboratory, Richland, WA 99352, USA

12 <sup>2</sup> Guana Tolomato Matanzas National Estuarine Research Reserve, Ponte Vedra Beach, FL 32082,  
13 USA

14 <sup>3</sup> Lake Superior National Estuarine Research Reserve, University of Wisconsin Madison, Division  
15 of Extension, Superior, WI 54880, USA

16 <sup>4</sup> San Francisco State University, Estuary and Ocean Science Center, Tiburon, CA 94920, USA

17 <sup>5</sup> School of Biological Sciences, Washington State University, Pullman, WA 99164, USA

18

19 \***Corresponding authors:** *Anna B. Turetcaia* [anna.turetcaia@pnnl.gov](mailto:anna.turetcaia@pnnl.gov) and *Emily B. Graham*  
20 [emily.graham@pnnl.gov](mailto:emily.graham@pnnl.gov)

21

22 ***Abstract***

23           Estuaries are subject to frequent stressors, including elevated nutrient loading and extreme  
24 hydrologic events, which impact water quality and disrupt ecosystem stability and health. The  
25 capacity of estuaries to resist changes in function in response to precipitation events is a key  
26 component of maintaining estuarine health in our changing climate. However, generalizable  
27 patterns in factors related to estuarine responses to extreme precipitation remain unknown. We  
28 investigate physicochemical factors and land-use characteristics that are associated with ecological  
29 resistance to precipitation – broadly defined as the magnitude of ecosystem change induced by an  
30 event – in five disparate estuaries distributed across the continental United States. Using long-term  
31 meteorological and water quality data from the National Estuarine Research Reserve System along  
32 with land use/land cover and population data within watersheds, we examine relationships between  
33 the resistance index – a proxy for ecosystem stability calculated using dissolved oxygen – and  
34 physicochemical and urban land use characteristics on local-to-continental scales. Contrary to our  
35 initial hypothesis, we found that more urbanized estuaries were more resistant to precipitation  
36 events, and that water temperature, water column depth, nitrogen, and chlorophyll-*a* were related  
37 to resistance on a continental scale. However, these trends interacted with estuarine salinity and  
38 varied across individual estuaries; where we found additional relationships of resistance with  
39 salinity, turbidity, phosphate concentrations, N:P, and tree cover. Considering emerging stressors  
40 from new climatic scenarios and from urbanization, these results are important for representing  
41 the impacts of disturbances in large-scale models and for informing management decisions  
42 regarding estuarine water quality.

43 ***Introduction***

44 Estuaries are highly dynamic environments that often connect freshwater and saltwater  
45 systems, cycle organic matter and nutrients from land to oceans, and provide essential ecosystem  
46 services (Bianchi, 2007; He & Silliman, 2019). The function of estuarine ecosystems as unique  
47 sites for carbon and nutrient cycling, and habitats for macro- and micro-flora and fauna, relies on  
48 stability of a predictable range of dynamic processes like temperature fluctuations, hydrology and  
49 nutrient mixing. However, anthropogenic activities and extreme climatic events threaten estuarine  
50 ecosystem function (Kemp et al., 2009; Zhang et al., 2010). Predicted increases in urban population  
51 size and in the frequency and intensity of precipitation events highlight the urgency to understand  
52 the response of estuaries to new urban and climatic scenarios (Kyzar et al., 2021; Li et al., 2019;  
53 Martínez et al., 2007; Pickett et al., 2011). Yet, the factors that impact the response of urban  
54 estuaries to precipitation are not fully understood.

55 When combined with intense precipitation, watershed urbanization and associated changes  
56 in land use/land cover (LULC) (Grimm et al., 2008) often result in increases in stream hydrological  
57 flashiness (Gannon et al., 2022; Reisinger et al., 2017). Hydrological flashiness induces increased  
58 flow rates that cause changes in channel morphology (Booth & Jackson, 1997; Gregory, 2011;  
59 Leopold, 1968; Vietz et al., 2016), habitat destruction (Walsh et al., 2005), and disruption of  
60 microbial metabolic processes (Reisinger et al., 2017; Uehlinger, 2000). Flashiness can also  
61 drastically affect primary production – a regulatory component of dissolved oxygen (DO)  
62 dynamics in aquatic environments – through increases in flow velocity, transport of phytoplankton,  
63 sediment migration, and light limitation (Bernot et al., 2010; Fisher et al., 1982; McSweeney et  
64 al., 2017; Reisinger et al., 2017; Uehlinger, 2000).

65           While DO concentration is dynamic and depends on a myriad of biological, chemical, and  
66 physical processes, it is essential for many estuarine functions and has been widely used as an  
67 indicator for overall ecosystem health (Abdul-Aziz et al., 2007; Abdul-Aziz & Gebreslase, 2023;  
68 Chapra, 2008; Cox, 2003; Kannel et al., 2007; Zhi et al., 2021). Dissolved oxygen is critical to  
69 maintaining the life cycles of macro- and micro-fauna, for example, and supports the  
70 biogeochemical cycling of carbon and nutrients by serving as a terminal electron acceptor  
71 (Bernhardt et al., 2018; Chapra, 2008; Zarnetske et al., 2012). Built areas in particular have been  
72 previously connected to degradation of aquatic DO concentrations, along with many other water  
73 quality parameters (Bernhardt et al., 2008; Chang, 2005; Freeman et al., 2019; Vietz et al., 2016).  
74 Given the tight link between aquatic DO, land use, and diverse ecosystem functions, DO is an  
75 important indicator of estuarine health.

76           In addition to impacts on DO, extreme precipitation events are often associated with excess  
77 nitrogen (N) delivery and changes in salinity, particularly for waterways adjacent to urban-type  
78 LULC (Walsh et al., 2005). Nitrogen is central to mediating metabolic processes across a wide  
79 range of ecosystems and land covers (Mulholland et al., 2008; Schindler, 1977; S. V. Smith, 1984;  
80 Vitousek & Howarth, 1991). It is particularly important for primary production in aquatic  
81 ecosystems because many phytoplankton species are N-limited (Evans & Seemann, 1989;  
82 Howarth, 1988; Vitousek & Howarth, 1991). Further, extreme precipitation events are often  
83 associated with influx of freshwater (i.e., runoff) and/or saltwater (i.e., storm surges) into estuaries,  
84 which changes salinity, can induce stratification and hypoxia, and impact ecosystem metabolic  
85 functions (Rabalais et al., 2010; Wetz & Yoskowitz, 2013; J. Zhang et al., 2010). However,  
86 depending on the temporal and spatial scales of evaluation, the reported trends of estuarine  
87 responses to precipitation and salinity changes can be conflicting.

88 Commonalities in responses to major precipitation events across disparate estuaries can  
89 help to project long-term estuary health under progressive urbanization and more extreme climate  
90 events; but they have been difficult to decipher. This is, in part, due to variation in how the complex  
91 and interconnected dynamics within estuaries respond to precipitation, even at local scales. While  
92 Ombadi & Varadharajan (2022) report contrasting effects of urbanization on salinity during flood  
93 events when regional climate is considered, a continental-scale study by Kaushal et al. (2018)  
94 suggests that anthropogenic activity is associated with increasing salinity in waterways. However,  
95 the later study recognizes that regional, climatic, LULC, and geologic variabilities also influence  
96 salinization patterns. Similarly, continental-scale evaluations showed that waterways within small  
97 watersheds appear consistently less flashy than those in large watersheds; and that there is a  
98 substantial amount of variability in these relationships at regional scale (Baker et al., 2004; Gannon  
99 et al., 2022; Hopkins et al., 2015; Poff et al., 2006). Such variation in relationships across scales  
100 may be particularly prevalent in ecosystems influenced by anthropogenic activities (Hopkins et  
101 al., 2015; Poff et al., 2006), which demonstrates the importance of considering multiple spatial  
102 scales in understanding estuarine responses to changes in precipitation patterns and watershed land  
103 use.

104 We aim to uncover generalizable patterns of responses to large precipitation events across  
105 five disparate estuaries spanning a gradient of urbanization and physicochemical properties. Using  
106 DO as an indicator of ecosystem health as per (Abdul-Aziz et al., 2007; Abdul-Aziz & Gebreslase,  
107 2023), we evaluate estuary resistance to precipitation – defined here as the ability of estuaries to  
108 maintain stability in DO concentration (Isbell et al., 2015; Lake, 2013; McCluney et al., 2014;  
109 Pimm, 1984; Utz et al., 2016; Van Meerbeek et al., 2021) – in the context of physicochemical  
110 factors and land-use characteristics at: 1) the continental-scale (i.e., across all estuaries); 2) across

111 estuaries grouped by salinity; and 3) within each estuary. We hypothesize that urbanization  
112 decreases estuarine resistance to precipitation, and further that relationships of resistance with  
113 physicochemical and land-use factors will diverge with spatial scale and differences in ambient  
114 salinity. This study is essential for understanding how ongoing changes in climate and urbanization  
115 conditions influence estuarine ecosystem health.

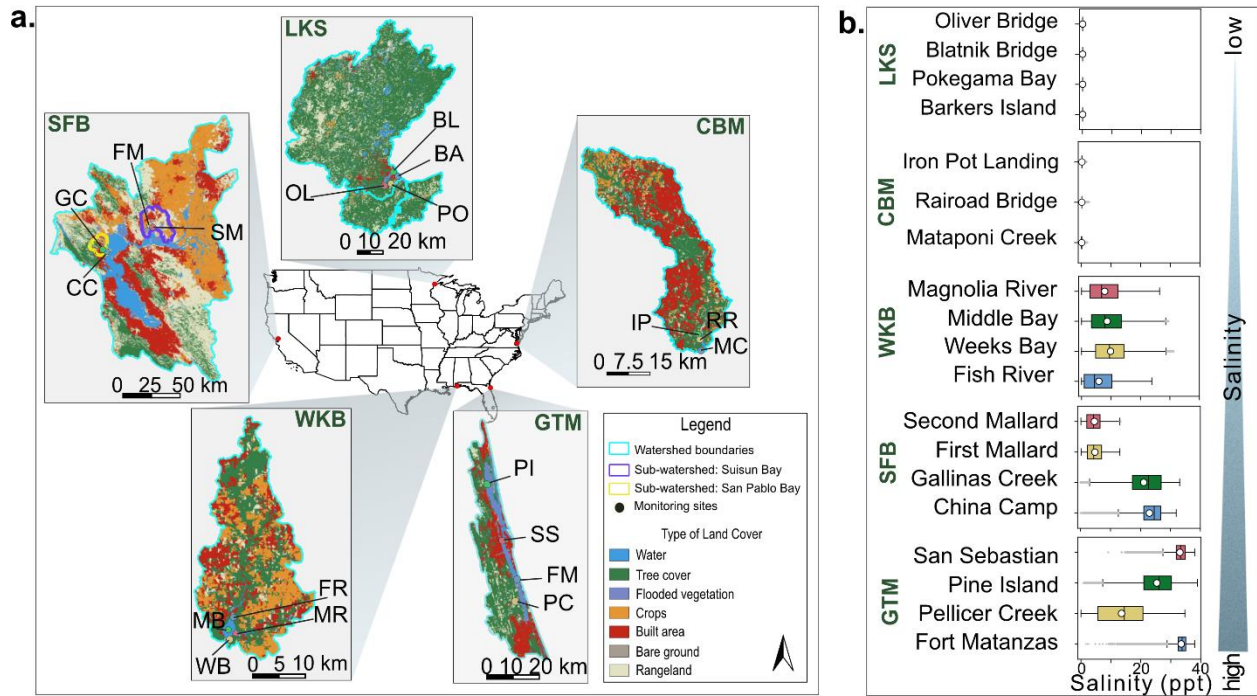
116

## 117 *Methods*

### 118 **Dataset Description.**

119 We used long-term water quality monitoring data from five estuaries in the National  
120 Estuarine Research Reserve System (NERRS, 2023) to understand factors associated with their  
121 resistance to precipitation events. Lake Superior (LKS), WI; Chesapeake Bay Maryland (CBM),  
122 MD (Jug Bay only); Guana Tolomato Matanzas (GTM), FL; Weeks Bay (WKB), AL; and San  
123 Francisco Bay (SFB), CA span climatic zones, land uses, and salinity (range from 0.1 to 35 ppt)  
124 (Fig. 1, Table 1). Across all estuaries, there were a total of 19 monitoring locations (3 at CBM, and  
125 4 at LKS, GTM, WKB, and SFB).

126



127

128 **Fig. 1.** Selected National Estuarine Research Reserve (NERR) stations. a) Map of monitoring  
 129 locations and land use/land cover within associated watersheds at Lake Superior (LKS) NERR,  
 130 Chesapeake Bay, Maryland (CBM) NERR, Guana Tolomato Matanzas (GTM) NERR, Weeks Bay  
 131 (WKB) NERR, and San Francisco Bay (SFB) NERR. b) Salinity from 2012 to 2022 for each  
 132 monitoring location at each NERR (all  $n > 150,000$ ). Boxes indicate interquartile range. Means  
 133 are shown in black-and-white circles. Black lines indicate medians.

134

135 **Table 1:** Land use/land cover (LULC) and population density in each estuary within 10-km to  
 136 water quality and nutrient monitoring locations.

LULC class	Estuary and % area by LULC class

	<i>LKS</i>	<i>CBM</i> <i>(Jug Bay)</i>	<i>GTM</i>	<i>WKB</i>	<i>SFB</i>	
					<i>(San Pablo Bay) CC, GC</i>	<i>(Suisun Bay) FM, SM</i>
Water	10.43	2.30	8.58	4.85	5.04	3.59
Tree cover	58.78	53.72	45.11	38.52	26.91	1.16
Flooded vegetation	0.88	1.37	13.04	0.05	1.4	21.33
Crops	0.19	4.63	0.19	30.36	18.05	19.67
Built area	18.84	27.19	23.99	19.33	31.65	21.87
Bare ground	0.06	0.25	0.26	0.1	0.11	1.17
Rangeland	9.82	10.53	8.82	6.76	16.47	31.2
Surface area and population estimates						
Area (km <sup>2</sup> )	488.7	218.2	645.6	213.0	105.01	205.86
Estimated population within the	71,111	49,291	148,557	17,404	48,161	100,582



area (ppl)						
Population density (ppl km <sup>-2</sup> )	145	225	230	81	458	488
LULC definitions per Esri (Karra et al., 2021)						
<p><i>Water</i> – areas where water was present throughout the year. Excludes man-made structures like docks</p> <p><i>Tree cover</i> – vegetation with closed/dense canopy <math>\geq 15</math> meters.</p> <p><i>Flooded vegetation</i> – areas with intermixing of water and vegetation flooded seasonally or predominantly throughout the year.</p> <p><i>Crops</i> – human planted vegetation (cereals, grasses, and corps) that are not at tree height.</p> <p><i>Built area</i> – human made structures like roads, railroad networks, parking spaces, industrial and residential buildings.</p> <p><i>Bare ground</i> – areas dominated by rocks, soil, sand (i.e. desert) with sparse to no vegetation throughout the year.</p> <p><i>Rangeland</i> – homogeneous grasses, mixes of vegetation below tree-height with rocks and soil, clearings in the forests.</p>						

137

138 To assess the relationships between resistance and urbanization, we used LULC data at 10-

139 meter resolution from available in Esri (2017-2020) (Karra et al., 2021) and population density

140 data at 100-meter resolution from World Population Hub (Bondarenko et al., 2020) (Table 1). We

141 analyzed LULC and population density using QGIS 3.30.3 (QGIS Development Team, 2023)

142 equipped with a semi-automatic classification plug-in. For SFB NERR, we used 10-km proximity  
143 zones from San Pablo and Suisun embayments to quantify LULC and population density as is  
144 conventionally done at this watershed due to different hydrologic dynamics within each ebayment.

145 All data were collected using NERRS standard operating procedures. Briefly, water  
146 column DO (corrected for temperature and salinity), temperature, conductivity, pH, turbidity,  
147 salinity, and depth were measured at 15-min intervals using synchronized YSI-EXO2  
148 multiparameter sondes. Meteorological conditions, including precipitation, were also measured at  
149 15-min intervals using NERRS standard weather station instrumentation.  $\text{PO}_4^{3-}$ ,  $\text{NO}_3^-$ ,  $\text{NH}_4^+$ ,  $\text{NO}_2^-$   
150 and chlorophyll-*a* (Chl-*a*) were measured monthly from grab samples and analyzed in the lab  
151 (NERRS, 2023). Samples for nutrients were filtered in the field through 0.7  $\mu\text{m}$  glass-fiber filters  
152 and analyzed following U.S. Environmental Protection Agency (EPA) methods (O'Dell, 1996b,  
153 1996a; U.S. EPA., 1993a). For Chl-*a* analysis, the samples were collected as whole water, then  
154 filtered onto 0.45  $\mu\text{m}$  glass-filters and processed following APHA, 2001 and U.S. EPA., 1993b  
155 methods. We omitted all data flagged as 'suspect' or 'out of range'.

156 Additionally, we calculated water column depth as the sum of measured water depth plus  
157 the distance between the sonde and sediment bed (Table S1). We also calculated the sum of  $\text{NO}_3^-$   
158 ,  $\text{NO}_2^-$ , and  $\text{NH}_4^+$  to assess dissolved inorganic nitrogen (DIN) concentrations and the ratio of DIN  
159 to  $\text{PO}_4^{3-}$  (hereafter, N:P).

160

### 161 **Determination of major precipitation events.**

162 Because hydrologic dynamics and related estuarine functions can vary dramatically with  
163 annual weather conditions, we first selected one 'wet' and one 'dry' year for each estuary using  
164 precipitation records from nearby airports. The purpose of selecting events from years with

165 disparate rainfall patterns was to encompass the maximum range of variability in expected  
166 estuarine resistance to precipitation. Following Murrell et al. (2018), we calculated the long-term  
167 interquartile range (IQR, 1990-2020) of total monthly precipitation for each estuary and then  
168 selected relatively wet/dry years based on the number of months plotting above/below IQR and  
169 total annual precipitation. Possible wet and dry years were further filtered based on the  
170 completeness of NERRS data available for each estuary (Fig. S1). Long-term precipitation records  
171 included: Duluth International, Washington Reagan International, Jacksonville International,  
172 Birmingham Airport, and San Francisco International airports available from the National Center  
173 for Environmental Information.

174 Further, we selected major precipitation events within each wet and dry year by plotting  
175 daily precipitation using data from NERR meteorological stations (Fig. S2). Specifically, because  
176 the definition of ‘major’ precipitation events is hard to quantify and it varies across estuaries, we  
177 first considered hurricanes, tropical storms, Nor’easters, and other major storm events noted within  
178 NERR metadata sheets when selecting precipitation events. For example, at GTM we focused on  
179 tropical storms Colin, Julia, and Hermine, hurricanes Matthew and Irma, and two Nor'easters  
180 (Table S2). Data availability was a second consideration – we removed possible events for which  
181 there was a substantial amount of missing data. Lastly, because metabolic and hydrologic  
182 processes vary across seasons, we chose to focus on warm season events, with the exception of  
183 San Francisco Bay where most precipitation occurs in the cool season, but seasonal temperature  
184 fluctuations are generally lower than in other systems (Fig. S2 and S3, Table S2).

185

186 **Calculation of estuarine resistance.**

187 To understand physicochemical and urban land-use characteristics associated with  
188 estuarine responses to precipitation events, we calculated the resistance index described in Orwin  
189 & Wardle (2004). The resistance index is a normalized parameter ( $-1$  to  $+1$ ) describing the  
190 magnitude of shift in a response variable from an initial condition. It has been used across a wide  
191 variety of ecosystems and response variables, including aquatic ecosystems (Thayne et al., 2022,  
192 2023; Tsai et al., 2011). It is calculated as:

193  $Resistance = 1 - \frac{2|D_0|}{(C_0 + |D_0|)}$  (eq. 1)

194  
195 where,  $C_0$  = concentration of the response variable pre-disturbance, and  $D_0$  = difference between  
196 the concentration of the response variable pre- and post-disturbance ( $P_0$ ) (i.e.,  $D_0 = C_0 - P_0$ ).

197 While the resistance index is indicative of the ability of a system to maintain its pre-  
198 disturbance state, we emphasize that it is a normalized value that does not in itself convey  
199 information about overall estuarine health. An index value of  $+1$  indicates the highest possible  
200 resistance. Index values between  $0$  and  $1$  show that the magnitude of response variable shift is less  
201 than the magnitude of the baseline (i.e.,  $|D_0| \leq C_0$ ). A resistance index of  $0$  indicates that the shift  
202 if the response variable is equivalent to the magnitude of the baseline (i.e.,  $|D_0| = C_0$ ), whereas  
203 index values between  $< 0$  and  $-1$  reflect that change in the response variable is greater than the  
204 magnitude of the baseline (i.e.,  $|D_0| > C_0$ ). Overall, index values closer to  $1$  indicate more resistant  
205 systems (Orwin & Wardle, 2004). Because it is a normalized value, the resistance index enables  
206 the comparison of the amount of change induced by disturbance across vastly different estuaries.  
207 In parallel, it is also useful to consider the absolute value of the response variable (in this case DO)  
208 pre- and post-disturbance, which conveys information on the ambient state of an estuary and the  
209 directionality of its response to the disturbance. We therefore present  $C_0$  and  $P_0$  (Fig. 2a-e, Table

210 S3) to define differences in DO within and across estuaries, as well as the resistance index, which  
211 pairs  $C_0$  and  $P_0$  values for the same event (Fig. 2f-j), to understand the ecosystem stability within  
212 and across estuaries after precipitation.

213 Because DO is critical to myriad functions that regulate the health of aquatic ecosystems  
214 (Abdul-Aziz et al., 2007; Abdul-Aziz & Gebreslase, 2023; Caffrey, 2004; Mulholland et al., 2001;  
215 Murrell et al., 2018; Odum, 1956) and because ecosystem metabolism is virtually impossible to  
216 model in tidal systems due to bi-directional flow (Loken et al., 2021); we used temperature and  
217 salinity adjusted DO concentration ( $\text{mg L}^{-1}$ ) to calculate the resistance index. Additionally, the  
218 resistance index is highly sensitive to the researcher-defined baseline and post-disturbance time  
219 periods that are used to calculate  $C_0$  and  $D_0$ . Therefore, we calculated  $C_0$  as average DO  
220 concentration during a manually-curated timespan preceding each precipitation event (~24 hours  
221 to 6 days, without precipitation) (Fig. S4, Table S2). The timespan for estimating  $P_0$  was also  
222 manually selected in the context of each event, defined here as the maximum displacement from  
223  $C_0$  during and after the event (Fig. S4, Table S2).

224

## 225 **Statistical analysis.**

226 To compare resistance, nutrient concentrations, and concentrations of DO pre- and post-  
227 precipitation within and between estuaries, we used ANOVA with post-hoc Tukey HSD or  
228 Kruskal-Wallis test, as appropriate based on the Shapiro-Wilk normality test.

229 To test associations of specific physicochemical and land-use factors with estuarine  
230 resistance to precipitation, we used linear regressions at continental and local scales independently  
231 (i.e., all estuaries combined vs. within each individual estuary) and within salinity-based groups  
232 (i.e., using a threshold of average annual salinity less than or above 10 ppt). We used annual mean

233 values for continental-scale and salinity-based regressions because monthly sampling intervals of  
234 lab-based measurements did not always correspond with selected precipitation events. This resulted  
235 in two data points per monitoring location. While not directly associated with any particular  
236 precipitation event, associations of annualized differences in nutrients and Chl-*a* with resistance  
237 values in a given year carry valuable information about how the ambient conditions of the system  
238 can impact an estuary's response to precipitation. This knowledge is essential for deriving and  
239 testing hypotheses that describe why a certain estuary may respond to a storm event in a particular  
240 way. For local-scale regressions (i.e., within individual estuaries) involving sensor-based  
241 measurements, we attempted to provide as much resolution as possible into specific events. We  
242 therefore used values averaged over event-specific time periods for sensor measurements and  
243 annualized values for lab-based assays when analyzing local results. Values averaged over event-  
244 specific time periods were matched with corresponding event-based resistance index resulting in  
245 a data point per precipitation event per each monitoring station. Annualized values were matched  
246 with mean resistance index calculated within the year resulting in two data points per monitoring  
247 location. We did not include LULC and population density as predictors of resistance at individual  
248 estuaries because of the close proximity of some monitoring locations to one another (< 800 m).

249 Statistical analyses were performed in Python 3.10.11 using `scipy.stats`,  
250 `statsmodels.stats.multicomp.pairwise_tukeyhsd`, and `seaborn.regplot` packages.

251

## 252 ***Results***

### 253 **Land use/land cover and nutrient concentrations across estuaries.**

254 Data describing LULC and population density for all estuaries are shown in Table 1. Both  
255 embayments of the SFB had higher percentages of urban-type land characteristics (e.g., built area)

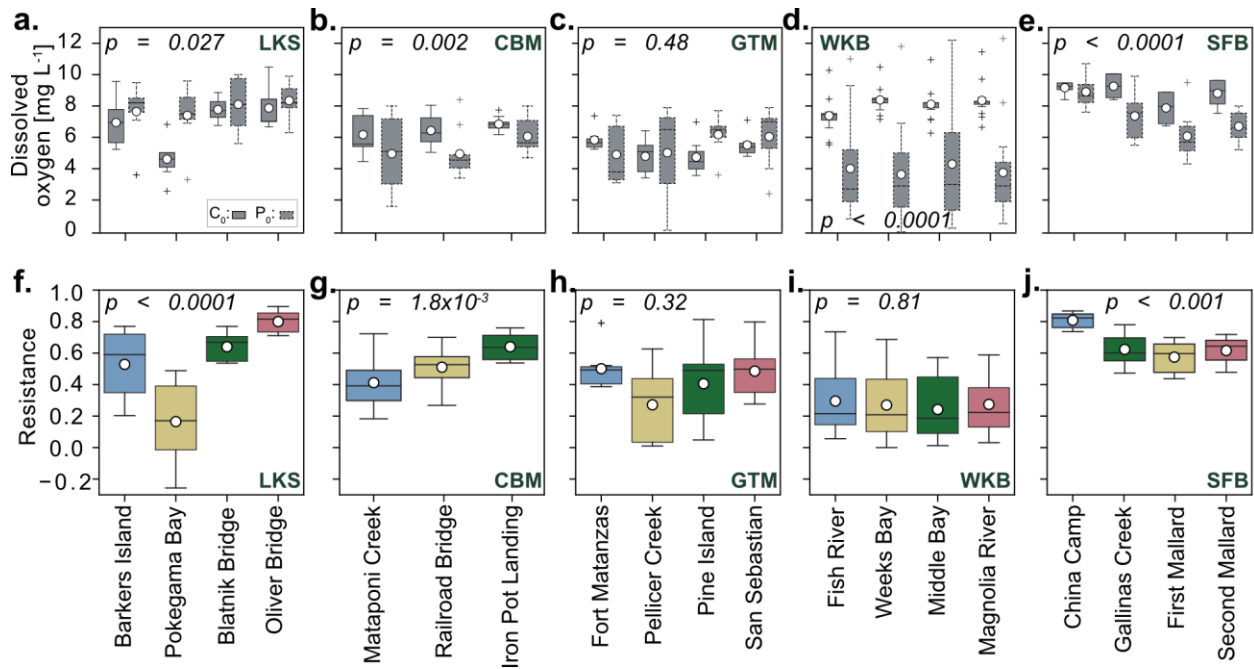
256 and population density than any other estuary, followed by CBM (Table 1). Agricultural land was  
257 more prevalent at WKB (30.36%) compared to other estuaries. GTM and LKS had more mixed  
258 LULC, with high proportions of tree cover. With regard to nutrient concentrations, SFB and CBM  
259 had high DIN concentrations compared to LKS and GTM ( $p < 0.01$ ). Mean DIN values at all SFB  
260 and CBM monitoring locations were  $> 0.504 \text{ mg-N L}^{-1}$  versus  $< 0.16 \text{ mg-N L}^{-1}$  at LKS and GTM  
261 (Fig. S5). Phosphate concentrations were the highest at SFB (mean across all monitoring locations  
262  $= 0.135 \text{ mg-P L}^{-1}$ ,  $SD = 0.08$ ), means at all other estuaries  $< 0.03 \text{ mg-P L}^{-1}$ ,  $p < 0.001$ , Fig. S5).  
263 Overall, mean N:P across LKS, CBM, GTM, WKB, and SFB estuaries were 28.04 ( $SD = 28.08$ ),  
264 26.56 ( $SD = 10.75$ ), 2.84 ( $SD = 0.91$ ), 83.82 ( $SD = 55.27$ ), and 5.10 ( $SD = 1.4$ ), respectively (Fig.  
265 S6), with GTM and SFB indicating N limiting conditions based on a 16N:1P Redfield ratio  
266 (Redfield, 1934).

267

268 **Changes in dissolved oxygen and resistance to precipitation across estuaries and monitoring**  
269 **locations.**

270 DO concentrations pre- and post-precipitation differed across all estuaries, when  
271 evaluating the overall trends (pre- ( $C_0$ ):  $F = 45.6$ ,  $p < 0.0001$ ; and post- ( $P_0$ ):  $F = 17.1$ ,  $p < 0.0001$ ,  
272 Fig. 2a-e). Across all large precipitation events (i.e., non-specific to an event), SFB had the highest  
273 pre-precipitation DO concentration of all estuaries. Generally, at SFB and CBM (more urban) and  
274 at WKB (more agricultural), DO declined following precipitation ( $p < 0.01$ ). At LKS, precipitation  
275 events significantly increased DO concentration ( $F = 5.1$ ,  $p = 0.027$ ). There was no significant  
276 difference between the overall pre- and post-precipitation DO concentrations at GTM ( $F = 0.5$ ,  $p$   
277  $= 0.48$ ).

278 Resistance also differed across estuaries ( $F = 21.6$ ,  $df_1 = 4$ ,  $df_2 = 172$ ,  $p < 0.0001$ , Fig 2).  
 279 SFB monitoring locations had the highest mean resistance to precipitation (mean = 0.68), while  
 280 monitoring locations at LKS were the least resistant to precipitation (mean = 0.47). Within  
 281 individual estuaries, resistance varied across monitoring locations at LKS ( $F = 13.9$ ,  $df_1 = 3$ ,  $df_2 =$   
 282  $= 24$ ,  $p < 0.0001$ ), CBM ( $F = 7.9$ ,  $df_1 = 2$ ,  $df_2 = 27$ ,  $p < 0.01$ ), and SFB ( $F = 10.2$ ,  $df_1 = 3$ ,  $df_2 =$   
 283  $27$ ,  $p < 0.001$ ) but was not significantly different between monitoring locations within GTM ( $F =$   
 284  $3.5$ ,  $df = 3$ ,  $p = 0.32$ ), WKB ( $F = 0.9$ ,  $df = 3$ ,  $p = 0.81$ ) (Fig. 2f-j). Resistance was most variable  
 285 across monitoring locations at LKS (-0.26 to 0.89) and least variable across locations at WKB (0  
 286 to 0.73).  
 287



288  
 289 **Fig. 2.** Variation in pre- and post-disturbance distribution of dissolved oxygen and resistance  
 290 within individual estuaries. Boxes show the quartiles of the dataset, and the whiskers show the rest  
 291 of the distribution. Means are shown in white circles, and medians are shown in black solid lines.  
 292 *P*-values are at the top of each panel. a-e) Distribution of dissolved oxygen concentrations prior to



293 (C<sub>0</sub>, solid boxes) and post (P<sub>0</sub>, dashed boxes) precipitation. f-j) Resistance index across monitoring  
294 locations at: Lake Superior (LKS) NERR (all n = 7), Chesapeake Bay (CBM) NERR (all n = 10),  
295 Guana Tolomato-Matanzas (GTM) NERR (all n = 7), Weeks Bay (WKB) NERR (all n = 15), San  
296 Francisco Bay (SFB) NERR (n = 8 except Second Mallard (SM) n = 7).

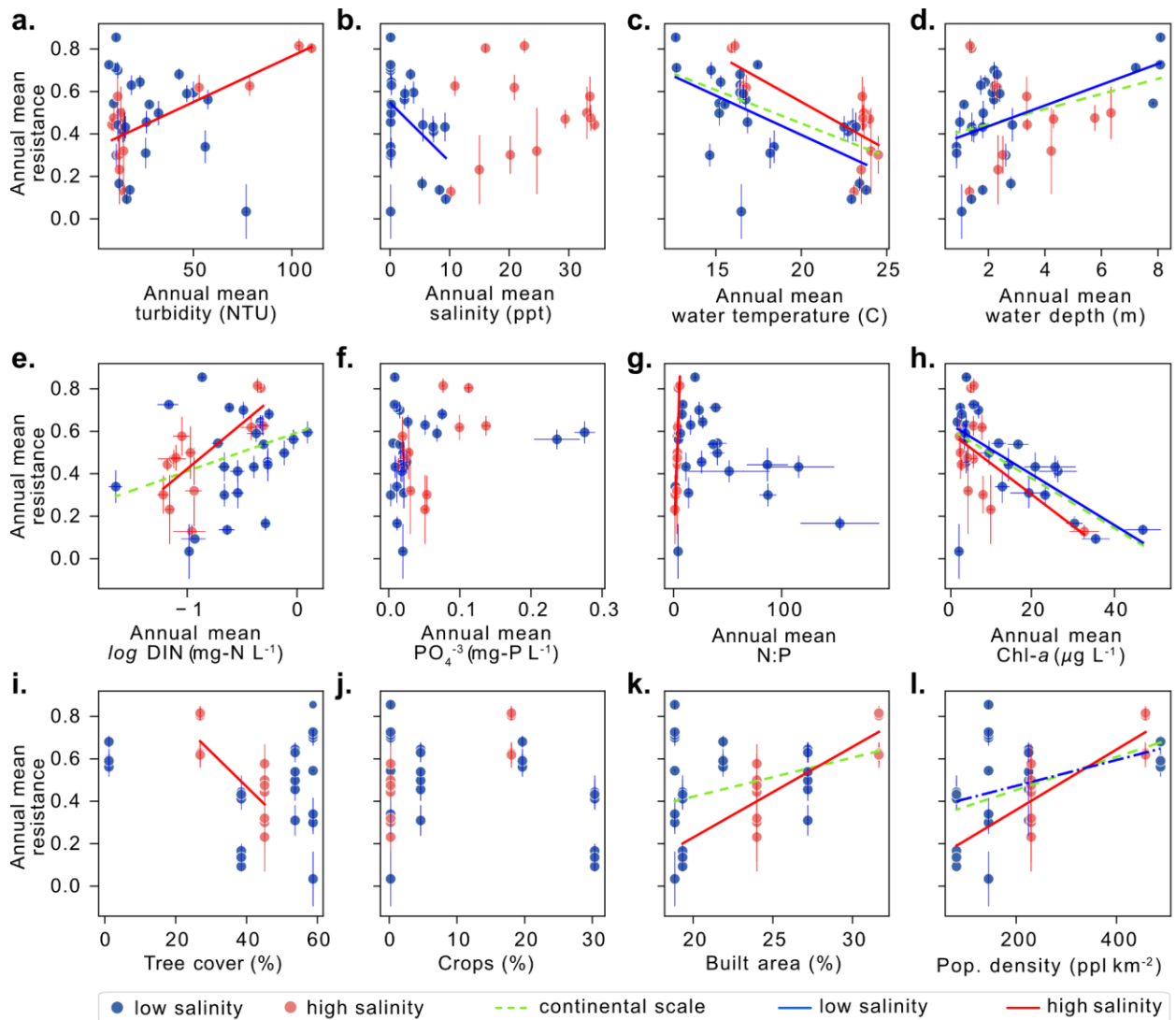
297

298 **Continental, salinity-based, and local relationships of resistance with physicochemical**  
299 **factors, land use/land cover, and population density.**

300 When data from the five estuaries were considered together (i.e., continental-scale), we  
301 found significant positive relationships of annual mean resistance with water column depth ( $p =$   
302  $0.027$ ;  $R^2 = 0.13$ ), log(DIN) ( $p = 0.031$ ;  $R^2 = 0.12$ ), percent built area ( $p = 0.02$ ;  $R^2 = 0.14$ ), and  
303 population density ( $p = 0.001$ ;  $R^2 = 0.27$ ); and significant negative relationships to water  
304 temperature ( $p = 0.0001$ ;  $R^2 = 0.35$ ) and Chl-*a* ( $p < 0.0001$ ;  $R^2 = 0.39$ ) (Fig. 3, Table S4).

305 When grouped by salinity, estuarine resistance to precipitation was more tightly correlated  
306 to physicochemical and land-use factors (Fig. 3, Table S4). Within ‘low-salinity’ estuaries, mean  
307 resistance was positively related with depth of the water column ( $p = 0.006$ ;  $R^2 = 0.29$ ), which is  
308 consistent with the trend observed on continental-scale; and negatively related to annual mean  
309 salinity ( $p = 0.029$ ;  $R^2 = 0.19$ ), a relationship not found on continental-scale. Within ‘high-salinity’  
310 estuaries, mean resistance showed positive relationships to annual mean log(DIN) ( $p = 0.004$ ;  $R^2$   
311  $= 0.55$ ) and to percent built area ( $p = 0.0002$ ,  $R^2 = 0.73$ ), which also was consistent with  
312 continental-scale results. Observations present in ‘high-salinity’ estuaries but absent from  
313 continental-scale evaluations included negative relationships of mean resistance with tree cover ( $p$   
314  $= 0.011$ ;  $R^2 = 0.46$ ), and negative relationships to N:P ( $p < 0.0001$ ;  $R^2 = 0.81$ ) and turbidity ( $p =$   
315  $0.001$ ,  $R^2 = 0.63$ ). Additionally, mean resistance in both low- and high-salinity groups was

316 positively related to population density ( $p = 0.051$ ;  $R^2 = 0.16$ , and  $p = 0.0002$ ;  $R^2 = 0.73$ ,  
 317 respectively), and negatively related to water temperature ( $p = 0.001$ ;  $R^2 = 0.38$ , and  $p = 0.002$ ;  
 318  $R^2 = 0.6$ , respectively) and Chl-*a* ( $p = 0.0002$ ,  $R^2 = 0.46$ , and  $p = 0.044$ ;  $R^2 = 0.32$ , respectively).  
 319 The temperature and Chl-*a* trends were consistent with continental-scale observations. Generally,  
 320 ‘low-salinity’ estuaries showed fewer relationships of mean resistance with annual mean  
 321 physicochemical factors, LULC, and population density compared to ‘high-salinity’ estuaries.  
 322



323

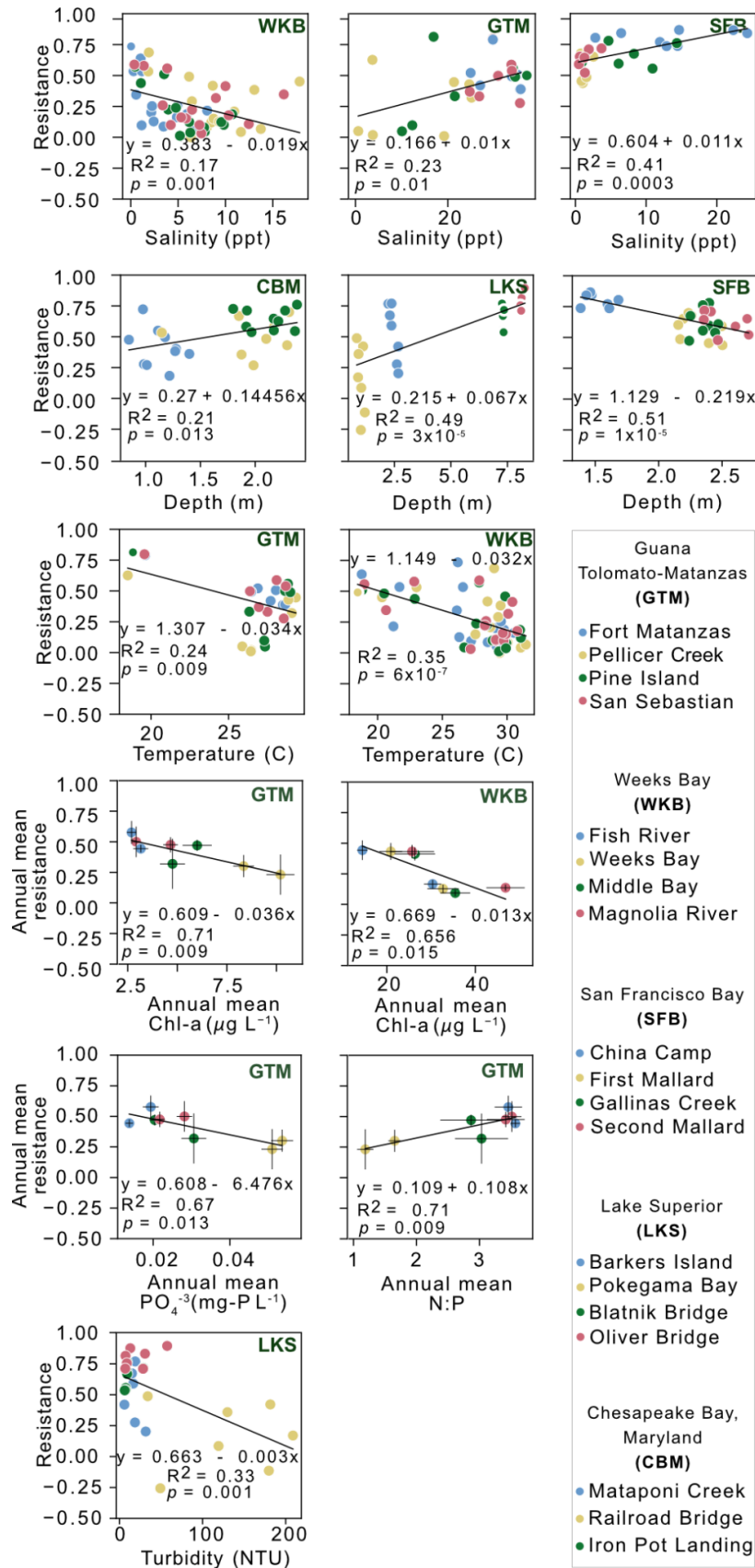
324 **Fig. 3.** Relationships of continental-scale and salinity-based resistance with physicochemical  
325 factors, land use/land cover, and population density. Continental-scale regressions considered all  
326 monitoring locations across all estuaries. Significant relationships ( $p < 0.05$ ) are shown in black,  
327 red, and blue for continental-scale, high-salinity estuaries, and low-salinity estuaries, respectively.  
328 Standard errors of the mean are shown in vertical and horizontal lines. Both salinity-based and  
329 continental-scale regression analysis use mean resistance values to correlate with annual mean  
330 turbidity, salinity, water temperature, water column depth, nutrients, N:P, and chlorophyll-*a* (Chl-  
331 *a*). The LULC parameters and population density were used from within the 10-km radius  
332 adjoined to the monitoring locations. Please refer to Table S4 for resulting statistics.

333

334 At local scales (i.e., within each estuary), resistance was related to some physicochemical  
335 factors that were not observed in continental-scale or salinity-based relationships. Moreover, the  
336 number, strength, and trends of relationships between local-scale resistance and physicochemical  
337 factors varied substantially across estuaries (Fig. 4, Figs. S7, S8). Resistance at GTM had the most  
338 relationships to physicochemical factors. It was negatively related to water temperature ( $p = 0.009$ ;  
339  $R^2 = 0.24$ ),  $\text{PO}_4^{3-}$  ( $p = 0.013$ ;  $R^2 = 0.67$ ) and Chl-*a* concentrations ( $p = 0.009$ ;  $R^2 = 0.71$ ); and  
340 positively related to salinity and N:P ( $p = 0.01$ ,  $R^2 = 0.23$ , and  $p = 0.009$ ;  $R^2 = 0.71$ , respectively).  
341 In contrast, at CBM, resistance was related only to water column depth (positive,  $p = 0.013$ ;  $R^2 =$   
342  $0.21$ ). At LKS, resistance was positively related to water column depth ( $p < 0.0001$ ;  $R^2 = 0.49$ ),  
343 and negatively related to turbidity ( $p = 0.001$ ;  $R^2 = 0.33$ ). At WKB, relationships of resistance with  
344 water temperature, salinity, and Chl-*a* concentrations were all negative ( $p < 0.0001$ ,  $R^2 = 0.35$ ;  $p$   
345  $= 0.001$ ,  $R^2 = 0.17$ ; and  $p = 0.015$ ,  $R^2 = 0.66$ , respectively). At SFB, resistance was negatively  
346 related to water column depth ( $p < 0.0001$ ;  $R^2 = 0.51$ ), which opposed the general trend, and

347 positively related to salinity ( $p = 0.0003$ ;  $R^2 = 0.41$ ). There was no overarching relationship  
348 between resistance and total precipitation amount of each event, except for a significant but weak  
349 negative relationship at GTM estuary ( $p = 0.026$ ,  $R^2 = 0.18$ , Fig. S9). Additional relationships  
350 between physicochemical parameters within estuaries are available in Fig. S10.

351

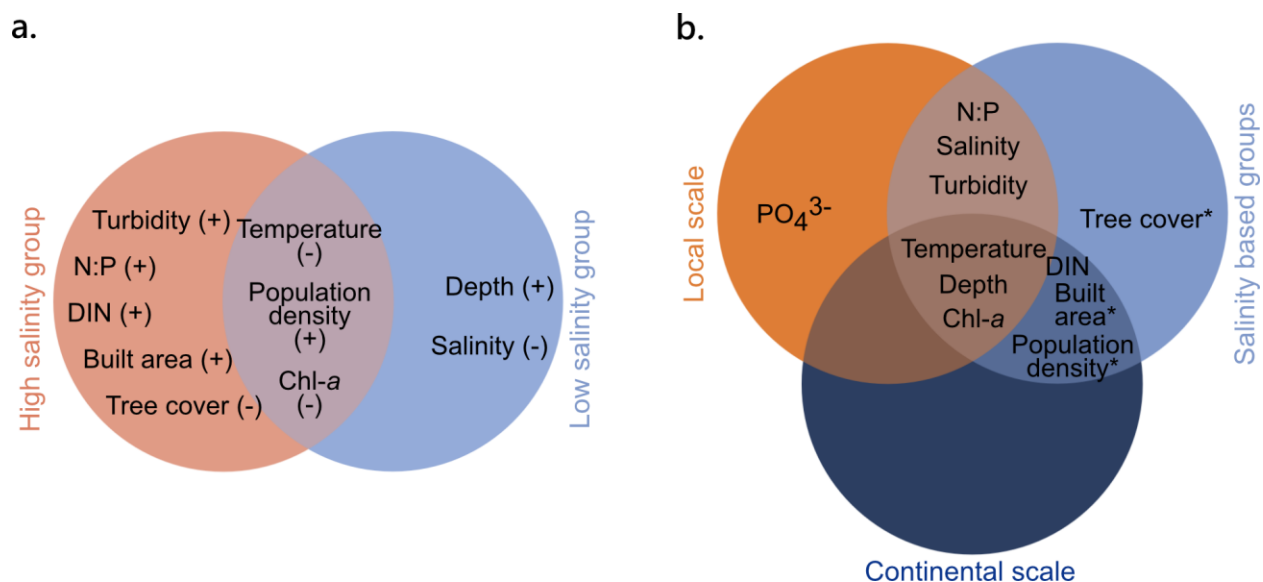


353 **Fig. 4.** Relationships between resistance and physicochemical factors for each estuary. National  
354 Estuarine Reserve System (NERR) estuary abbreviations: Lake Superior (LKS) NERR,  
355 Chesapeake Bay, Maryland (CBM) NERR, Guana Tolomato Matanzas (GTM) NERR, Weeks Bay  
356 (WKB) NERR, and San Francisco Bay (SFB) NERR. Significant correlations ( $p < 0.05$ ) are shown  
357 with black lines. Standard errors of the mean are shown in vertical and horizontal lines for  
358 relationships using annual means for chlorophyll-*a* (Chl-*a*),  $\text{PO}_4^{3-}$ , and N:P. For additional results  
359 see Figs. S7 and S8.

360

361 In summary, some relationships of estuarine resistance with physicochemical factors and  
362 urban land use appeared to be more universal while others varied across scales (Fig. 5). For  
363 instance, resistance was related to water temperature, water column depth, and Chl-*a* across  
364 continental- and local-scales, and within salinity-based estuary groups. Dissolved inorganic N,  
365 percent built area, and population density were all related to resistance at the continental scale and  
366 in salinity-based group. Both local and salinity-based evaluations revealed correlations of N:P,  
367 salinity, and turbidity with resistance to precipitation. Unique relationships included  $\text{PO}_4^{3-}$  at the  
368 local scale (GTM only) and tree cover in ‘high-salinity’ estuaries.

369



370

371 **Fig. 5.** Cross-scale relationships of estuarine resistance with physicochemical factors and land-use  
 372 characteristics. a) Venn diagram of resistance relationships to physicochemical factors and land-  
 373 use characteristics in high- vs. low-salinity estuaries. Positive or negative relationships are  
 374 indicated with ‘+’ and ‘-’ respectively. b) Venn diagram of resistance relationships with  
 375 physicochemical and land-use factors in continental, local, and salinity-based groups. Estuarine  
 376 resistance with land use/land cover and population density marked with asterisks (\*) were not  
 377 evaluated at local-scale due to overlap in the spatial domains of some monitoring locations.

378

379 **Discussion**

380 Understanding patterns in estuarine responses to precipitation is important for predicting  
 381 the impacts of urbanization and climate change on estuaries as a whole. Previous studies have  
 382 shown that patterns identified at large scales may not been applicable across different climatic  
 383 conditions, regional geology, and other ecosystem factors (Baker et al., 2004; Gannon et al., 2022;  
 384 Hopkins et al., 2015; Kaushal et al., 2018; Ombadi & Varadharajan, 2022; Poff et al., 2006). Our  
 385 results underscore the importance of cross-scale evaluations that can elucidate commonalities in

386 estuarine response to precipitation, as well as variability in the factors associated with resistance  
387 to precipitation across individual estuaries.

388 We show that while relationships between estuarine resistance, urbanization, and DIN may  
389 prevail at the continental-scale, they may not correspond to resistance in individual estuaries. This  
390 is because local resistance is associated with myriad specific factors in addition to many factors  
391 identified at larger scales. Also, in contrast to our overarching hypothesis, we find that urbanized  
392 estuaries tend to have higher resistance than more pristine estuaries. These results could suggest  
393 that the effects of watershed urbanization may impact estuarine stability by providing a mechanism  
394 that allows estuaries responding to major precipitation events to withstand large shifts in DO  
395 concentrations. Alternatively, urbanization may disturb the baseline DO to an extent where even a  
396 major precipitation event would not produce a significant shift in DO, making the system appear  
397 highly resistant.

398

### 399 **Dissolved oxygen dynamics differ in estuaries with urban or agricultural land use/land cover**

400 There are vast differences in geometry, circulation, and hydrologic conditions among  
401 urbanized estuaries and/or estuaries surrounded by agricultural land in this study. Yet, they  
402 exhibited similar patterns in DO concentration in response to precipitation. Precipitation generally  
403 reduced DO concentrations at WKB, SFB, and CBM (Fig. 2a-e). Simultaneously, the estuary with  
404 the least amount of urbanized LULC – LKS – overall, experienced an increase in DO concentration  
405 following precipitation.

406 While a wide range of physical factors can impact DO concentrations in estuaries including  
407 channel geometry and river discharge (Kemp & Boynton, 1980; Raymond et al., 2012; Raymond  
408 & Cole, 2001), wind (Scully, 2010; Zheng et al., 2024), and circulation (Raimonet & Cloern,



409 2017); urban estuaries in particular often experience a combination of these processes. Urban  
410 estuaries often serve as basins for wastewater treatment outflows, which can supply continued  
411 freshwater discharge and nutrients when river discharge is low. Both urban and agriculturally  
412 influenced estuaries are prone to increased nutrient loading during and shortly after precipitation  
413 events (Chapin et al., 2004; Costanzo et al., 2003; Mallin et al., 2009), which impacts primary  
414 production and microbial metabolism and may lead to declines in DO concentrations (e.g., algal  
415 blooms).

416

417 **Urbanization and inorganic nitrogen correspond with elevated resistance to precipitation at**  
418 **the continental-scale.**

419 Higher precipitation resistance index in the most urbanized estuaries, and overarching  
420 relationships of urban LULC with resistance across all estuaries, suggest that estuaries within  
421 urban watersheds may be able to better withstand changes to DO following precipitation (Figs. 2-  
422 3). This result contradicts our hypothesis that urban estuaries should show low resistance to  
423 precipitation because of greater physical and chemical disturbances, like flashiness, streambed  
424 scouring, and N loading, which alter hydrology, turbidity, and interfere with metabolism  
425 (Bernhardt et al., 2008; Groffman et al., 2004; Hession et al., 2003; Hopkinson & Vallino, 1995;  
426 Walsh et al., 2005).

427 However, it is possible that watershed urbanization could equip estuaries with a set of  
428 controls that mitigate precipitation impacts on DO. For instance, an increase in flashiness in  
429 waterways would increase flow velocity and reaeration of the water column in estuaries (Raymond  
430 et al., 2012; Raymond & Cole, 2001) and contribute to phytoplankton removal via transport or  
431 turbidity-driven light attenuation (Caffrey, 2004; Pennock & Sharp, 1986). This impact may be

432 particularly important for estuaries whose baseline conditions are influenced by algal blooms,  
433 which induce large DO fluctuations by overproducing DO during the day and severely depleting  
434 DO at night (Chapin et al., 2004; Ni et al., 2020). Such control for overgrowth of phytoplankton  
435 would help maintain DO near baseline. Supporting this explanation, turbidity-driven limitations  
436 on phytoplankton were previously reported for the SFB estuary (Cloern, 1987). We also found  
437 positive and negative relationships of turbidity and Chl-*a*, respectively, with built area and  
438 population density (Fig. S11).

439 Watershed urbanization is often related to high N export to estuarine environments (Bettez  
440 et al., 2015; Hopkinson & Vallino, 1995; Reisinger et al., 2016). Here, estuarine N concentrations  
441 were related to urbanization and also were a major predictor of resistance at the continental-scale  
442 (Figs. 3 and S11). While nutrient loading is a significant problem for urban aquatic environments  
443 (Beman et al., 2005; Bernot et al., 2010; Black et al., 2011; Mulholland et al., 2008), more  
444 moderate levels of N support basic metabolic functions, including healthy levels of phytoplankton  
445 growth (Camenzind et al., 2018; Foldager Pedersen & Borum, 1996; Gobler et al., 2006; Howarth,  
446 1988; Howarth & Marino, 2006; Larsen & Harvey, 2017; Moore & Hunt, 2013; Schimel &  
447 Bennett, 2004; Sullivan et al., 2014; Vitousek & Howarth, 1991; Woodland et al., 2015; Q. Zhang  
448 et al., 2021). The link between estuary N concentrations and phytoplankton is important because  
449 primary producers critically influence water column DO concentrations, reflected by gross primary  
450 productivity in models of aquatic metabolism (Odum, 1956). Moreover, relationships of resistance  
451 with N and urbanization were particularly evident in high-salinity estuaries where we found  
452 positive relationships of resistance with N:P and built area (Fig. 3). Nitrogen limitation of  
453 processes such as microbial metabolism and phytoplankton growth is prevalent in coastal marine  
454 systems (Elser et al., 2007; Guildford & Hecky, 2000; Paerl, 2018; Paerl & Piehler, 2008).

455 Therefore, we propose that N delivery following precipitation may have a short-term stabilizing  
456 effect on some estuaries.

457

458 **Water column depth, temperature, and Chl-*a* relate with resistance across all scales.**

459 We found generalizable patterns (across all scales), in which resistance was positively  
460 related to water column depth and negatively related to water temperature and Chl-*a* (Figs. 3-5).  
461 As discussed above, phytoplankton dynamics appear to be an important factor in regulating DO in  
462 response to disturbance, which is consistent with results previously reported by (Thayne et al.,  
463 2023), and this is further underscored by the existence of a relationship between Chl-*a* and  
464 resistance across continental, salinity-based, and local analyses.

465 Through dilution, deeper estuaries should have a greater capacity to resist hydrologic  
466 changes in response to precipitation, for instance by attenuating the influx of oxygen-saturated rain  
467 water; nutrient loading; turbulence; and water-atmosphere gas exchange. Similarly, deep estuaries  
468 have longer equilibration time with environmental conditions and less diel variability in  
469 parameters like temperature (Caissie, 2006; Macan, 1958), which also affects diel and seasonal  
470 DO dynamics, possibly resulting in more stable baseline DO concentrations and more moderate  
471 responses to precipitation. Deeper estuaries can also be associated with urbanization, which also  
472 shows high resistance in this study, because shifts towards more urban and agricultural LULC can  
473 deepen estuarine channels through increased runoff, sediment transport, hydrological flashiness,  
474 channel dredging, and/or other anthropogenic activities (O'Driscoll et al., 2010; Simon & Rinaldi,  
475 2006; Walsh et al., 2005). Therefore, water column depth appears to be a critical factor in  
476 regulating the responses of estuaries to precipitation.

477           Lastly, because temperature controls various chemical and biological processes that impact  
478 DO availability (e.g., microbial growth, oxygen solubility), many studies have focused on the  
479 impact of rising temperature on DO dynamics in estuaries (Apple et al., 2006; Caffrey, 2003;  
480 Caffrey et al., 2014). Highlighted results link climate change to thermal pollution of aquatic  
481 systems following rain events (Zahn et al., 2021) and show connections of elevated global  
482 temperatures with decreased primary production (Song et al., 2018). As such, estuaries with  
483 elevated ambient temperatures may have a decreased capacity to resist disturbance from  
484 precipitation relative to estuaries with more moderate temperatures.

485

486 **High variability in factors associated with resistance at local scales.**

487           The contrasting relationships between physicochemical factors and resistance across  
488 monitoring locations in individual estuaries highlight substantial fine-scale variation in  
489 precipitation response (Fig. 4). For example, resistance at CBM is related to one factor (water  
490 column depth), while at GTM, resistance is related to five factors. The variability in factors  
491 associated with resistance suggests that individual estuaries may need to consider factors beyond  
492 water temperature, water column depth, and Chl-*a* in water-quality management and conservation  
493 strategies. For instance, Chl-*a* and dissolved inorganic phosphorus have been shown to respond to  
494 storms in some estuaries more than in others due to differences in light limitation, grazing, and  
495 nutrient concentrations (Chen et al., 2015; Cloern, 2001; Cloern & Jassby, 2010; N. Dix et al.,  
496 2013; N. G. Dix et al., 2008; Liao et al., 2021; M. Zhang et al., 2022). Likewise, water temperature  
497 and salinity also have variable responses to precipitation (Buelo et al., 2023; Chen et al., 2015; N.  
498 G. Dix et al., 2008), leading to differences in biological processes and phytoplankton activity in  
499 different estuaries (Apple et al., 2008). While there are myriad potential estuary-specific

500 interactions that may result in different responses to stressors, our results highlight that system-  
501 variability is important when identifying parameters involved in estuarine resistance to  
502 precipitation. We also acknowledge that other scales of investigation (e.g., regional) could  
503 introduce additional insight into the predictors of estuarine resistance.

504

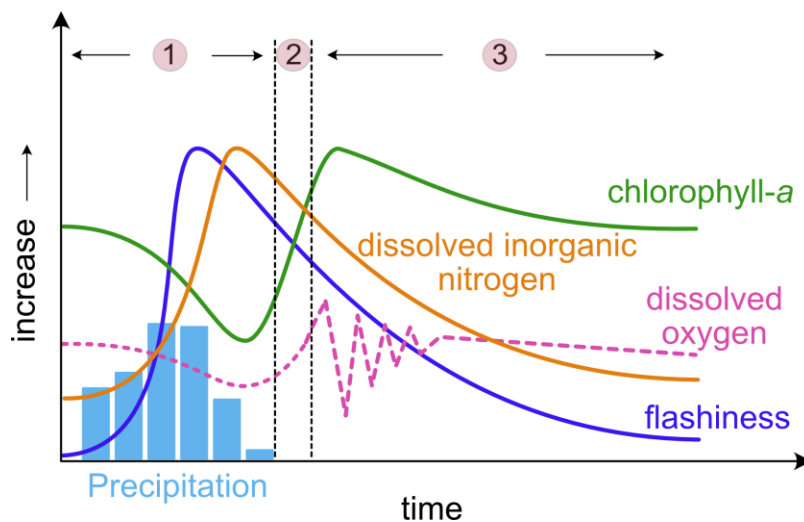
### 505 **Possible explanations for elevated precipitation resistance in more urban estuaries**

506         Based on our findings that urban estuaries may be more resistant to precipitation than more  
507 natural estuaries, we ponder if watershed urbanization may be accompanied by short-term  
508 adaptation mechanisms that help estuaries offset the effects of precipitation. In particular, we  
509 question if hydrological flashiness and N delivery associated with precipitation could influence  
510 phytoplankton and DO concentrations to have a temporary (hours to days) beneficial effect on DO  
511 stability in more urban estuaries (Fig. 6).

512         Dissolved oxygen availability in estuaries is tightly linked to phytoplankton, which in turn  
513 responds to N availability (Evans & Seemann, 1989; Howarth, 1988; Vitousek & Howarth, 1991).  
514 Nitrogen may be particularly important for high-salinity estuaries, which are often N-limited  
515 (Howarth & Marino, 2006; Paerl, 2018) and are comparatively more restrictive for phytoplankton  
516 development due to growth-limiting salt concentrations (Flameling & Kromkamp, 1994; Mo et  
517 al., 2021; Russell et al., 2023). Also, because watershed urbanization is often accompanied by  
518 increased flashiness during rain events (B. K. Smith & Smith, 2015), it follows that in urban  
519 estuaries precipitation may help remove excess phytoplankton through increased flow velocity.  
520 Simultaneously, storm runoff may deliver the necessary N concentrations that help phytoplankton  
521 biomass recover and temporarily restore baseline DO in urban estuaries, where N loadings tend to

522 be higher (Bettez et al., 2015; Reisinger et al., 2016). Collectively, these processes could lead to  
 523 higher resistance to precipitation in urban estuaries that may be more responsive to N inputs.

524 However, we note that high-resolution measurements surrounding precipitation events, as  
 525 well as careful evaluations of phytoplankton, salinity, and N surrounding the events are needed to  
 526 distinguish effects on DO concentrations pre- and post-precipitation. We also highlight the  
 527 importance of evaluating N as chemical species, because of known inhibitory effects of excess  
 528 ammonium on nitrate uptake by phytoplankton, which reduces algal growth (Dugdale et al., 2007;  
 529 Parker et al., 2012). Moreover, system dependencies on groundwater discharge as a driver of  
 530 nutrient dynamics and control on phytoplankton and DO (Brookfield et al., 2021; Kornelsen &  
 531 Coulibaly, 2014) as well as phytoplankton dependencies on microbial community structure (Cheng  
 532 et al., 2021) should also be considered. Lastly, we underline that this study encompasses a  
 533 relatively short time frame (i.e., hours to days) and should not be extrapolated to longer time scales.  
 534 Excess phytoplankton growth that causes eutrophication, often referred to as algal blooms, occurs  
 535 over longer time frames, even in high-salinity estuaries (Anderson et al., 2021).



536  
 537 **Fig. 6.** Conceptual model for interplay of precipitation, flashiness, dissolved inorganic nitrogen,  
 538 phytoplankton, and dissolved oxygen in urban estuaries. 1) Precipitation induces flashiness (dark

539 blue curve) which leads to an immediate decrease in phytoplankton (green curve) and a shift in  
540 dissolved oxygen (pink curve). Simultaneously, precipitation promotes influx of excess dissolved  
541 inorganic nitrogen (orange curve) which leads to 2) a positive response in concentration of  
542 phytoplankton and, on short-term, prevents a large shift in DO away from its baseline  
543 concentration. Overtime, the influx of excess dissolved inorganic nitrogen is followed by 3)  
544 elevated phytoplankton concentrations and severe disturbance of dissolved oxygen baseline.

545

546         Alternatively, we also consider if baseline DO concentrations in urban estuaries are already  
547 disturbed to such an extent that additional disturbances, such as major precipitation events, cause  
548 minimal further disruption. For example, urbanization itself can promote large diel DO  
549 fluctuations as suggested by (Gold et al., 2020), and if a precipitation event induces fluctuations  
550 that are similar in magnitude, post-precipitation DO concentrations will not deviate significantly  
551 from baseline conditions. Under such a scenario, urban estuaries will appear more resistant to  
552 precipitation events compared to more natural estuaries.

553

## 554 *Conclusions*

555         In light of increasing urbanization and emerging climatic scenarios, cross-scale evaluations  
556 of the responses of estuaries to precipitation events are imperative for developing effective  
557 management strategies. We find that urban estuaries are more resistant to precipitation and the  
558 depth of the water column, water temperature, and Chl-*a* are generalizable cross-scale predictors  
559 for estuarine resistance. However, across different scales, we find that system variability results in  
560 additional factors that are important to consider when managing the responses to major  
561 precipitations events of individual estuaries. Based on our results, we propose a conceptual model

562 for future investigation in which the impact of urbanization on the interplay of N and  
563 phytoplankton dynamics may help estuaries resist the effects of major precipitation events on  
564 estuarine health. However, high-resolution water quality and nutrient data surrounding  
565 precipitation events, along with careful considerations of local variabilities and models for system  
566 responses to precipitation, are needed to help elucidate the underlying mechanisms for high  
567 resistance of urban estuaries. This study serves as a platform for improvement of guidelines and  
568 predictive capabilities addressing system response to future climatic and urbanization scenarios.

569

### 570 *Acknowledgements*

571 This material is based upon work supported by the U.S. Department of Energy, Office of Science,  
572 Biological and Environmental Research program Early Career award to EBG. The work was  
573 performed by Pacific Northwest National Laboratory, operated by Battelle Memorial Institute for  
574 the U.S. Department of Energy under Contract DE-AC05-76RL01830. We thank the National  
575 Estuarine Research Reserve System (NERRS), supported by awards from the Office for Coastal  
576 Management, National Oceanographic and Atmospheric Administration (NOAA), and Drs. Kyle  
577 Derby and Scott Phipps from Chesapeake Bay, Maryland NERR and Weeks Bay NERR,  
578 respectively, for maintaining water quality monitoring stations and providing publicly available  
579 data upon which this publication is based. The authors report no conflicts of interests.



580 **References**

- 581 Abdul-Aziz, O. I., & Gebreslase, A. K. (2023). Emergent Scaling of Dissolved Oxygen (DO) in  
582 Freshwater Streams Across Contiguous USA. *Water Resources Research*, 59(2),  
583 e2022WR032114. <https://doi.org/10.1029/2022WR032114>
- 584 Abdul-Aziz, O. I., Wilson, B. N., & Gulliver, J. S. (2007). Calibration and Validation of an  
585 Empirical Dissolved Oxygen Model. *Journal of Environmental Engineering*, 133(7), 698–  
586 710. [https://doi.org/10.1061/\(ASCE\)0733-9372\(2007\)133:7\(698\)](https://doi.org/10.1061/(ASCE)0733-9372(2007)133:7(698))
- 587 Anderson, D. M., Fensin, E., Gobler, C. J., Hoeglund, A. E., Hubbard, K. A., Kulis, D. M.,  
588 Landsberg, J. H., Lefebvre, K. A., Provoost, P., Richlen, M. L., Smith, J. L., Solow, A. R.,  
589 & Trainer, V. L. (2021). Marine harmful algal blooms (HABs) in the United States:  
590 History, current status and future trends. *Harmful Algae*, 102, 101975.  
591 <https://doi.org/10.1016/j.hal.2021.101975>
- 592 APHA. (2001). *Standard Methods for the Examination of Water and Wastewater*, (SM10200H)  
593 (20th ed.). United Book Press, Inc.
- 594 Apple, J. K., Giorgio, P. A. del, & Kemp, W. M. (2006). Temperature regulation of bacterial  
595 production, respiration, and growth efficiency in a temperate salt-marsh estuary. *Aquatic  
596 Microbial Ecology*, 43(3), 243–254. <https://doi.org/10.3354/ame043243>
- 597 Apple, J. K., Smith, E. M., & Boyd, T. J. (2008). Temperature, Salinity, Nutrients, and the  
598 Covariation of Bacterial Production and Chlorophyll-a in Estuarine Ecosystems. *Journal  
599 of Coastal Research*, 2008(10055), 59–75. <https://doi.org/10.2112/SI55-005.1>
- 600 Baker, D. B., Richards, R. P., Loftus, T. T., & Kramer, J. W. (2004). A New Flashiness Index:  
601 Characteristics and Applications to Midwestern Rivers and Streams1. *JAWRA Journal of  
602 the American Water Resources Association*, 40(2), 503–522.

- 603 <https://doi.org/10.1111/j.1752-1688.2004.tb01046.x>
- 604 Beman, M. J., Arrigo, K. R., & Matson, P. A. (2005). Agricultural runoff fuels large phytoplankton  
605 blooms in vulnerable areas of the ocean. *Nature*, 434(7030), Article 7030.  
606 <https://doi.org/10.1038/nature03370>
- 607 Bernhardt, E. S., Band, L. E., Walsh, C. J., & Berke, P. E. (2008). Understanding, Managing, and  
608 Minimizing Urban Impacts on Surface Water Nitrogen Loading. *Annals of the New York  
609 Academy of Sciences*, 1134, 61–96. <https://doi.org/10.1196/annals.1439.014>
- 610 Bernhardt, E. S., Heffernan, J. B., Grimm, N. B., Stanley, E. H., Harvey, J. W., Arroita, M.,  
611 Appling, A. P., Cohen, M. J., McDowell, W. H., Hall Jr., R. O., Read, J. S., Roberts, B. J.,  
612 Stets, E. G., & Yackulic, C. B. (2018). The metabolic regimes of flowing waters.  
613 *Limnology and Oceanography*, 63(S1), S99–S118. <https://doi.org/10.1002/lno.10726>
- 614 Bernot, M. J., Sobota, D. J., Hall Jr, R. O., Mulholland, P. J., Dodds, W. K., Webster, J. R., Tank,  
615 J. L., Ashkenas, L. R., Cooper, L. W., Dahm, C. N., Gregory, S. V., Grimm, N. B.,  
616 Hamilton, S. K., Johnson, S. L., Mcdowell, W. H., Meyer, J. L., Peterson, B., Poole, G. C.,  
617 Valett, H. M., ... Wilson, K. (2010). Inter-regional comparison of land-use effects on  
618 stream metabolism. *Freshwater Biology*, 55(9), 1874–1890.  
619 <https://doi.org/10.1111/j.1365-2427.2010.02422.x>
- 620 Bettez, N. D., Duncan, J. M., Groffman, P. M., Band, L. E., O’neil-dunne, J., Kaushal, S. S., Belt,  
621 K. T., & Law, N. (2015). Climate Variation Overwhelms Efforts to Reduce Nitrogen  
622 Delivery to Coastal Waters. *Ecosystems*, 18(8), 1319–1331.  
623 <https://doi.org/10.1007/s10021-015-9902-9>
- 624 Bianchi, T. S. (2007). *Biogeochemistry of Estuaries*. Oxford University Press, USA.
- 625 Black, R. W., Moran, P. W., & Frankforter, J. D. (2011). Response of algal metrics to nutrients

- 626 and physical factors and identification of nutrient thresholds in agricultural streams.  
627 *Environmental Monitoring and Assessment*, 175(1), 397–417.  
628 <https://doi.org/10.1007/s10661-010-1539-8>
- 629 Bondarenko, M., Kerr, D., Sorichetta, A., & Tatem, A. (2020). *Census/projection-disaggregated*  
630 *gridded population datasets for 189 countries in 2020 using Built-Settlement Growth*  
631 *Model (BSGM) outputs* [Dataset]. University of Southampton.  
632 <https://doi.org/10.5258/SOTON/WP00684>
- 633 Booth, D. B., & Jackson, C. R. (1997). Urbanization of Aquatic Systems: Degradation Thresholds,  
634 Stormwater Detection, and the Limits of Mitigation1. *JAWRA Journal of the American*  
635 *Water Resources Association*, 33(5), 1077–1090. [https://doi.org/10.1111/j.1752-](https://doi.org/10.1111/j.1752-1688.1997.tb04126.x)  
636 [1688.1997.tb04126.x](https://doi.org/10.1111/j.1752-1688.1997.tb04126.x)
- 637 Brookfield, A. E., Hansen, A. T., Sullivan, P. L., Czuba, J. A., Kirk, M. F., Li, L., Newcomer, M.  
638 E., & Wilkinson, G. (2021). Predicting algal blooms: Are we overlooking groundwater?  
639 *Science of The Total Environment*, 769, 144442.  
640 <https://doi.org/10.1016/j.scitotenv.2020.144442>
- 641 Buelo, C. D., Besterman, A. F., Walter, J. A., Pace, M. L., Ha, D. T., & Tassone, S. J. (2023).  
642 Quantifying Disturbance and Recovery in Estuaries: Tropical Cyclones and High-  
643 Frequency Measures of Oxygen and Salinity. *Estuaries and Coasts*.  
644 <https://doi.org/10.1007/s12237-023-01255-1>
- 645 Caffrey, J. M. (2003). Production, Respiration and Net Ecosystem Metabolism in U.S. Estuaries.  
646 In B. D. Melzian, V. Engle, M. McAlister, S. Sandhu, & L. K. Eads (Eds.), *Coastal*  
647 *Monitoring through Partnerships: Proceedings of the Fifth Symposium on the*  
648 *Environmental Monitoring and Assessment Program (EMAP) Pensacola Beach, FL*,

- 649 U.S.A., April 24–27, 2001 (pp. 207–219). Springer Netherlands.  
650 [https://doi.org/10.1007/978-94-017-0299-7\\_19](https://doi.org/10.1007/978-94-017-0299-7_19)
- 651 Caffrey, J. M. (2004). Factors controlling net ecosystem metabolism in U.S. estuaries. *Estuaries*,  
652 27(1), 90–101. <https://doi.org/10.1007/BF02803563>
- 653 Caffrey, J. M., Murrell, M. C., Amacker, K. S., Harper, J. W., Phipps, S., & Woodrey, M. S.  
654 (2014). Seasonal and Inter-annual Patterns in Primary Production, Respiration, and Net  
655 Ecosystem Metabolism in Three Estuaries in the Northeast Gulf of Mexico. *Estuaries and  
656 Coasts*, 37(1), 222–241. <https://doi.org/10.1007/s12237-013-9701-5>
- 657 Caissie, D. (2006). The thermal regime of rivers: A review. *Freshwater Biology*, 51(8), 1389–  
658 1406. <https://doi.org/10.1111/j.1365-2427.2006.01597.x>
- 659 Camenzind, T., Hättenschwiler, S., Treseder, K. K., Lehmann, A., & Rillig, M. C. (2018). Nutrient  
660 limitation of soil microbial processes in tropical forests. *Ecological Monographs*, 88(1), 4–  
661 21. <https://doi.org/10.1002/ecm.1279>
- 662 Chang, H. (2005). Spatial and Temporal Variations of Water Quality in the Han River and Its  
663 Tributaries, Seoul, Korea, 1993–2002. *Water, Air, and Soil Pollution*, 161(1), 267–284.  
664 <https://doi.org/10.1007/s11270-005-4286-7>
- 665 Chapin, T. P., Caffrey, J. M., Jannasch, H. W., Coletti, L. J., Haskins, J. C., & Johnson, K. S.  
666 (2004). Nitrate sources and sinks in Elkhorn Slough, California: Results from long-term  
667 continuous in situ nitrate analyzers. *Estuaries*, 27(5), 882–894.  
668 <https://doi.org/10.1007/BF02912049>
- 669 Chapra, S. C. (2008). *Surface Water-Quality Modeling*. Waveland Press.
- 670 Chen, N., Wu, Y., Chen, Z., & Hong, H. (2015). Phosphorus export during storm events from a  
671 human perturbed watershed, southeast China: Implications for coastal ecology. *Estuarine*,

- 672 *Coastal and Shelf Science*, 166, 178–188. <https://doi.org/10.1016/j.ecss.2015.03.023>
- 673 Cheng, Y., Bhoot, V. N., Kumbier, K., Sison-Mangus, M. P., Brown, J. B., Kudela, R., &  
674 Newcomer, M. E. (2021). A novel random forest approach to revealing interactions and  
675 controls on chlorophyll concentration and bacterial communities during coastal  
676 phytoplankton blooms. *Scientific Reports*, 11(1), 19944. [https://doi.org/10.1038/s41598-](https://doi.org/10.1038/s41598-021-98110-9)  
677 021-98110-9
- 678 Cloern, J. E. (1987). Turbidity as a control on phytoplankton biomass and productivity in estuaries.  
679 *Continental Shelf Research*, 7(11), 1367–1381. [https://doi.org/10.1016/0278-](https://doi.org/10.1016/0278-4343(87)90042-2)  
680 4343(87)90042-2
- 681 Cloern, J. E. (2001). Our evolving conceptual model of the coastal eutrophication problem. *Marine*  
682 *Ecology Progress Series*, 210, 223–253. <https://doi.org/10.3354/meps210223>
- 683 Cloern, J. E., & Jassby, A. D. (2010). Patterns and Scales of Phytoplankton Variability in  
684 Estuarine–Coastal Ecosystems. *Estuaries and Coasts*, 33(2), 230–241.  
685 <https://doi.org/10.1007/s12237-009-9195-3>
- 686 Costanzo, S. D., O’Donohue, M. J., & Dennison, W. C. (2003). Assessing the seasonal influence  
687 of sewage and agricultural nutrient inputs in a subtropical river estuary. *Estuaries*, 26(4),  
688 857–865. <https://doi.org/10.1007/BF02803344>
- 689 Cox, B. (2003). A review of currently available in-stream water-quality models and their  
690 applicability for simulating dissolved oxygen in lowland rivers. *The Science of The Total*  
691 *Environment*, 314–316, 335–377. [https://doi.org/10.1016/S0048-9697\(03\)00063-9](https://doi.org/10.1016/S0048-9697(03)00063-9)
- 692 Dix, N. G., Philips, E. J., & Gleeson, R. A. (2008). Water Quality Changes in the Guana Tolomato  
693 Matanzas National Estuarine Research Reserve, Florida, Associated with Four Tropical  
694 Storms. *Journal of Coastal Research*, 2008(10055), 26–37. <https://doi.org/10.2112/SI55->

695 008.1

696 Dix, N., Phlips, E., & Suscy, P. (2013). Factors Controlling Phytoplankton Biomass in a  
697 Subtropical Coastal Lagoon: Relative Scales of Influence. *Estuaries and Coasts*, 36(5),  
698 981–996. <https://doi.org/10.1007/s12237-013-9613-4>

699 Dugdale, R. C., Wilkerson, F. P., Hogue, V. E., & Marchi, A. (2007). The role of ammonium and  
700 nitrate in spring bloom development in San Francisco Bay. *Estuarine, Coastal and Shelf  
701 Science*, 73(1), 17–29. <https://doi.org/10.1016/j.ecss.2006.12.008>

702 Elser, J. J., Bracken, M. E. S., Cleland, E. E., Gruner, D. S., Harpole, W. S., Hillebrand, H., Ngai,  
703 J. T., Seabloom, E. W., Shurin, J. B., & Smith, J. E. (2007). Global analysis of nitrogen  
704 and phosphorus limitation of primary producers in freshwater, marine and terrestrial  
705 ecosystems. *Ecology Letters*, 10(12), 1135–1142. [https://doi.org/10.1111/j.1461-  
0248.2007.01113.x](https://doi.org/10.1111/j.1461-<br/>706 0248.2007.01113.x)

707 Evans, J. R., & Seemann, J. R. (1989). The allocation of protein nitrogen in the photosynthetic  
708 apparatus: Costs, consequences, and control. In W. R. Briggs (Ed.), *Photosynthesis* (pp.  
709 183–205). Alan R. Liss.

710 Fisher, S. G., Gray, L. J., Grimm, N. B., & Busch, D. E. (1982). Temporal Succession in a Desert  
711 Stream Ecosystem Following Flash Flooding. *Ecological Monographs*, 52(1), 93–110.  
712 <https://doi.org/10.2307/2937346>

713 Flameling, I. A., & Kromkamp, J. (1994). Responses of respiration and photosynthesis of  
714 *Scenedesmus protuberans* Fritsch to gradual and steep salinity increases. *Journal of  
715 Plankton Research*, 16(12), 1781–1791. <https://doi.org/10.1093/plankt/16.12.1781>

716 Foldager Pedersen, M., & Borum, J. (1996). Nutrient control of algal growth in estuarine waters.  
717 Nutrient limitation and the importance of nitrogen requirements and nitrogen storage

- 718 among phytoplankton and species of macroalgae. *Marine Ecology Progress Series*, 142,  
719 261–272. <https://doi.org/10.3354/meps142261>
- 720 Freeman, L. A., Corbett, D. R., Fitzgerald, A. M., Lemley, D. A., Quigg, A., & Steppe, C. N.  
721 (2019). Impacts of Urbanization and Development on Estuarine Ecosystems and Water  
722 Quality. *Estuaries and Coasts*, 42(7), 1821–1838. [https://doi.org/10.1007/s12237-019-](https://doi.org/10.1007/s12237-019-00597-z)  
723 00597-z
- 724 Gannon, J. P., Kelleher, C., & Zimmer, M. (2022). Controls on watershed flashiness across the  
725 continental US. *Journal of Hydrology*, 609, 127713.  
726 <https://doi.org/10.1016/j.jhydrol.2022.127713>
- 727 Gobler, C. J., Buck, N. J., Sieracki, M. E., & Sañudo-Wilhelmy, S. A. (2006). Nitrogen and silicon  
728 limitation of phytoplankton communities across an urban estuary: The East River-Long  
729 Island Sound system. *Estuarine, Coastal and Shelf Science*, 68(1), 127–138.  
730 <https://doi.org/10.1016/j.ecss.2006.02.001>
- 731 Gold, A., Thompson, S., Magel, C., & Piehler, M. (2020). Urbanization alters coastal plain stream  
732 carbon export and dissolved oxygen dynamics. *Science of The Total Environment*, 747,  
733 141132. <https://doi.org/10.1016/j.scitotenv.2020.141132>
- 734 Gregory, K. J. (2011). Wolman MG (1967) A cycle of sedimentation and erosion in urban river  
735 channels. *Geografiska Annaler* 49A: 385-395. *Progress in Physical Geography*, 35(6),  
736 831–841. <https://doi.org/10.1177/0309133311414527>
- 737 Grimm, N. B., Faeth, S. H., Golubiewski, N. E., Redman, C. L., Wu, J., Bai, X., & Briggs, J. M.  
738 (2008). Global Change and the Ecology of Cities. *Science*, 319(5864), 756–760.
- 739 Groffman, P. M., Law, N. L., Belt, K. T., Band, L. E., & Fisher, G. T. (2004). Nitrogen Fluxes and  
740 Retention in Urban Watershed Ecosystems. *Ecosystems*, 7(4), 393–403.

- 741 <https://doi.org/10.1007/s10021-003-0039-x>
- 742 Guildford, S. J., & Hecky, R. E. (2000). Total nitrogen, total phosphorus, and nutrient limitation  
743 in lakes and oceans: Is there a common relationship? *Limnology and Oceanography*, 45(6),  
744 1213–1223. <https://doi.org/10.4319/lo.2000.45.6.1213>
- 745 He, Q., & Silliman, B. R. (2019). Climate Change, Human Impacts, and Coastal Ecosystems in  
746 the Anthropocene. *Current Biology*, 29(19), R1021–R1035.  
747 <https://doi.org/10.1016/j.cub.2019.08.042>
- 748 Hession, W. C., Pizzuto, J. E., Johnson, T. E., & Horwitz, R. J. (2003). Influence of bank  
749 vegetation on channel morphology in rural and urban watersheds. *Geology*, 31(2), 147–  
750 150. [https://doi.org/10.1130/0091-7613\(2003\)031<0147:IOBVOC>2.0.CO;2](https://doi.org/10.1130/0091-7613(2003)031<0147:IOBVOC>2.0.CO;2)
- 751 Hopkins, K. G., Morse, N. B., Bain, D. J., Bettez, N. D., Grimm, N. B., Morse, J. L., Palta, M. M.,  
752 Shuster, W. D., Bratt, A. R., & Suchy, A. K. (2015). Assessment of Regional Variation in  
753 Streamflow Responses to Urbanization and the Persistence of Physiography.  
754 *Environmental Science & Technology*, 49(5), 2724–2732.  
755 <https://doi.org/10.1021/es505389y>
- 756 Hopkinson, C. S., & Vallino, J. J. (1995). The relationships among man's activities in watersheds  
757 and estuaries: A model of runoff effects on patterns of estuarine community metabolism.  
758 *Estuaries*, 18(4), 598–621. <https://doi.org/10.2307/1352380>
- 759 Howarth, R. W. (1988). Nutrient Limitation of Net Primary Production in Marine Ecosystems.  
760 *Annual Review of Ecology and Systematics*, 19, 89–110.
- 761 Howarth, R. W., & Marino, R. (2006). Nitrogen as the limiting nutrient for eutrophication in  
762 coastal marine ecosystems: Evolving views over three decades. *Limnology and*  
763 *Oceanography*, 51(1part2), 364–376. [https://doi.org/10.4319/lo.2006.51.1\\_part\\_2.0364](https://doi.org/10.4319/lo.2006.51.1_part_2.0364)



- 764 Isbell, F., Craven, D., Connolly, J., Loreau, M., Schmid, B., Beierkuhnlein, C., Bezemer, T. M.,  
765 Bonin, C., Bruelheide, H., de Luca, E., Ebeling, A., Griffin, J. N., Guo, Q., Hautier, Y.,  
766 Hector, A., Jentsch, A., Kreyling, J., Lanta, V., Manning, P., ... Eisenhauer, N. (2015).  
767 Biodiversity increases the resistance of ecosystem productivity to climate extremes.  
768 *Nature*, 526(7574), 574–577. <https://doi.org/10.1038/nature15374>
- 769 Kannel, P. R., Lee, S., Lee, Y.-S., Kanel, S. R., & Khan, S. P. (2007). Application of Water Quality  
770 Indices and Dissolved Oxygen as Indicators for River Water Classification and Urban  
771 Impact Assessment. *Environmental Monitoring and Assessment*, 132(1), 93–110.  
772 <https://doi.org/10.1007/s10661-006-9505-1>
- 773 Karra, K., Kontgis, C., Statman-Weil, Z., Mazzariello, J. C., Mathis, M., & Brumby, S. P. (2021).  
774 Global land use / land cover with Sentinel 2 and deep learning. *2021 IEEE International*  
775 *Geoscience and Remote Sensing Symposium IGARSS*, 4704–4707.  
776 <https://doi.org/10.1109/IGARSS47720.2021.9553499>
- 777 Kaushal, S. S., Likens, G. E., Pace, M. L., Utz, R. M., Haq, S., Gorman, J., & Grese, M. (2018).  
778 Freshwater salinization syndrome on a continental scale. *Proceedings of the National*  
779 *Academy of Sciences*, 115(4), E574–E583. <https://doi.org/10.1073/pnas.1711234115>
- 780 Kemp, W. M., & Boynton, W. R. (1980). Influence of biological and physical processes on  
781 dissolved oxygen dynamics in an estuarine system: Implications for measurement of  
782 community metabolism. *Estuarine and Coastal Marine Science*, 11(4), 407–431.  
783 [https://doi.org/10.1016/S0302-3524\(80\)80065-X](https://doi.org/10.1016/S0302-3524(80)80065-X)
- 784 Kemp, W. M., Testa, J. M., Conley, D. J., Gilbert, D., & Hagy, J. D. (2009). Temporal responses  
785 of coastal hypoxia to nutrient loading and physical controls. *Biogeosciences*, 6(12), 2985–  
786 3008. <https://doi.org/10.5194/bg-6-2985-2009>

- 787 Kornelsen, K. C., & Coulibaly, P. (2014). Synthesis review on groundwater discharge to surface  
788 water in the Great Lakes Basin. *Journal of Great Lakes Research*, 40(2), 247–256.  
789 <https://doi.org/10.1016/j.jglr.2014.03.006>
- 790 Kyzar, T., Safak, I., Cebrian, J., Clark, M. W., Dix, N., Dietz, K., Gittman, R. K., Jaeger, J.,  
791 Radabaugh, K. R., Roddenberry, A., Smith, C. S., Sparks, E. L., Stone, B., Sundin, G.,  
792 Taubler, M., & Angelini, C. (2021). Challenges and opportunities for sustaining coastal  
793 wetlands and oyster reefs in the southeastern United States. *Journal of Environmental*  
794 *Management*, 296, 113178. <https://doi.org/10.1016/j.jenvman.2021.113178>
- 795 Lake, P. S. (2013). Resistance, Resilience and Restoration. *Ecological Management &*  
796 *Restoration*, 14(1), 20–24. <https://doi.org/10.1111/emr.12016>
- 797 Larsen, L. G., & Harvey, J. W. (2017). Disrupted carbon cycling in restored and unrestored urban  
798 streams: Critical timescales and controls. *Limnology and Oceanography*, 62(S1), S160–  
799 S182. <https://doi.org/10.1002/lno.10613>
- 800 Leopold, L. B. (1968). Hydrology for urban land planning—A guidebook on the hydrologic effects  
801 of urban land use. In *Circular* (554). U.S. Geological Survey.  
802 <https://doi.org/10.3133/cir554>
- 803 Li, C., Zwiers, F., Zhang, X., Chen, G., Lu, J., Li, G., Norris, J., Tan, Y., Sun, Y., & Liu, M. (2019).  
804 Larger Increases in More Extreme Local Precipitation Events as Climate Warms.  
805 *Geophysical Research Letters*, 46(12), 6885–6891.  
806 <https://doi.org/10.1029/2019GL082908>
- 807 Liao, A., Han, D., Song, X., & Yang, S. (2021). Impacts of storm events on chlorophyll-a  
808 variations and controlling factors for algal bloom in a river receiving reclaimed water.  
809 *Journal of Environmental Management*, 297, 113376.

- 810 <https://doi.org/10.1016/j.jenvman.2021.113376>
- 811 Loken, L. C., Van Nieuwenhuysse, E. E., Dahlgren, R. A., Lenocho, L. E. K., Stumpner, P. R., Burau,  
812 J. R., & Sadro, S. (2021). Assessment of multiple ecosystem metabolism methods in an  
813 estuary. *Limnology and Oceanography: Methods*, 19(11), 741–757.  
814 <https://doi.org/10.1002/lom3.10458>
- 815 Macan, T. T. (1958). The temperature of a small stony stream. *Hydrobiologia*, 12(2), 89–106.  
816 <https://doi.org/10.1007/BF00034143>
- 817 Mallin, M. A., Johnson, V. L., & Ensign, S. H. (2009). Comparative impacts of stormwater runoff  
818 on water quality of an urban, a suburban, and a rural stream. *Environmental Monitoring  
819 and Assessment*, 159(1–4), 475–491. <https://doi.org/10.1007/s10661-008-0644-4>
- 820 Martínez, M. L., Intralawan, A., Vázquez, G., Pérez-Maqueo, O., Sutton, P., & Landgrave, R.  
821 (2007). The coasts of our world: Ecological, economic and social importance. *Ecological  
822 Economics*, 63(2–3), 254–272. <https://doi.org/10.1016/j.ecolecon.2006.10.022>
- 823 McCluney, K. E., Poff, N. L., Palmer, M. A., Thorp, J. H., Poole, G. C., Williams, B. S., Williams,  
824 M. R., & Baron, J. S. (2014). Riverine macrosystems ecology: Sensitivity, resistance, and  
825 resilience of whole river basins with human alterations. *Frontiers in Ecology and the  
826 Environment*, 12(1), 48–58. <https://doi.org/10.1890/120367>
- 827 McSweeney, J. M., Chant, R. J., Wilkin, J. L., & Sommerfield, C. K. (2017). Suspended-Sediment  
828 Impacts on Light-Limited Productivity in the Delaware Estuary. *Estuaries and Coasts*,  
829 40(4), 977–993. <https://doi.org/10.1007/s12237-016-0200-3>
- 830 Mo, Y., Peng, F., Gao, X., Xiao, P., Logares, R., Jeppesen, E., Ren, K., Xue, Y., & Yang, J. (2021).  
831 Low shifts in salinity determined assembly processes and network stability of  
832 microeukaryotic plankton communities in a subtropical urban reservoir. *Microbiome*, 9(1),

- 833 128. <https://doi.org/10.1186/s40168-021-01079-w>
- 834 Moore, T. L. C., & Hunt, W. F. (2013). Predicting the carbon footprint of urban stormwater  
835 infrastructure. *Ecological Engineering*, 58, 44–51.  
836 <https://doi.org/10.1016/j.ecoleng.2013.06.021>
- 837 Mulholland, P. J., Fellows, C. S., Tank, J. L., Grimm, N. B., Webster, J. R., Hamilton, S. K., Martí,  
838 E., Ashkenas, L., Bowden, W. B., Dodds, W. K., McDowell, W. H., Paul, M. J., & Peterson,  
839 B. J. (2001). Inter-biome comparison of factors controlling stream metabolism. *Freshwater  
840 Biology*, 46(11), 1503–1517. <https://doi.org/10.1046/j.1365-2427.2001.00773.x>
- 841 Mulholland, P. J., Helton, A. M., Poole, G. C., Hall, R. O., Hamilton, S. K., Peterson, B. J., Tank,  
842 J. L., Ashkenas, L. R., Cooper, L. W., Dahm, C. N., Dodds, W. K., Findlay, S. E. G.,  
843 Gregory, S. V., Grimm, N. B., Johnson, S. L., McDowell, W. H., Meyer, J. L., Valett, H.  
844 M., Webster, J. R., ... Thomas, S. M. (2008). Stream denitrification across biomes and its  
845 response to anthropogenic nitrate loading. *Nature*, 452(7184), Article 7184.  
846 <https://doi.org/10.1038/nature06686>
- 847 Murrell, M. C., Caffrey, J. M., Marcovich, D. T., Beck, M. W., Jarvis, B. M., & Hagy, J. D. (2018).  
848 Seasonal oxygen dynamics in a warm temperate estuary: Effects of hydrologic variability  
849 on measurements of primary production, respiration, and net metabolism. *Estuaries and  
850 Coasts: Journal of the Estuarine Research Federation*, 41(3), 690–707.  
851 <https://doi.org/10.1007/s12237-017-0328-9>
- 852 NERRS. (2023). *NOAA National Estuarine Research Reserve System (NERRS). System-wide  
853 Monitoring Program*. <https://cdmo.baruch.sc.edu/>
- 854 Ni, W., Li, M., & Testa, J. M. (2020). Discerning effects of warming, sea level rise and nutrient  
855 management on long-term hypoxia trends in Chesapeake Bay. *Science of The Total*

- 856 *Environment*, 737, 139717. <https://doi.org/10.1016/j.scitotenv.2020.139717>
- 857 O'Dell, J. W. (1996a). Determination Of Nitrate-Nitrite Nitrogen by Automated Colorimetry. In
- 858 *Methods for the Determination of Metals in Environmental Samples* (pp. 464–478).
- 859 Elsevier. <https://doi.org/10.1016/B978-0-8155-1398-8.50026-4>
- 860 O'Dell, J. W. (1996b). Determination of Phosphorus by Semi-Automated Colorimetry. In *Methods*
- 861 *for the Determination of Metals in Environmental Samples* (pp. 479–495). Elsevier.
- 862 <https://doi.org/10.1016/B978-0-8155-1398-8.50027-6>
- 863 O'Driscoll, M., Clinton, S., Jefferson, A., Manda, A., & McMillan, S. (2010). Urbanization Effects
- 864 on Watershed Hydrology and In-Stream Processes in the Southern United States. *Water*,
- 865 2(3), Article 3. <https://doi.org/10.3390/w2030605>
- 866 Odum, H. T. (1956). Primary Production in Flowing Waters. *Limnology and Oceanography*, 1(2),
- 867 102–117. <https://doi.org/10.4319/lo.1956.1.2.0102>
- 868 Ombadi, M., & Varadharajan, C. (2022). Urbanization and aridity mediate distinct salinity
- 869 response to floods in rivers and streams across the contiguous United States. *Water*
- 870 *Research*, 220, 118664. <https://doi.org/10.1016/j.watres.2022.118664>
- 871 Orwin, K. H., & Wardle, D. A. (2004). New indices for quantifying the resistance and resilience
- 872 of soil biota to exogenous disturbances. *Soil Biology and Biochemistry*, 36(11), 1907–
- 873 1912. <https://doi.org/10.1016/j.soilbio.2004.04.036>
- 874 Paerl, H. W. (2018). Why does N-limitation persist in the world's marine waters? *Marine*
- 875 *Chemistry*, 206, 1–6. <https://doi.org/10.1016/j.marchem.2018.09.001>
- 876 Paerl, H. W., & Piehler, M. F. (2008). Chapter 11—Nitrogen and Marine Eutrophication. In D. G.
- 877 Capone, D. A. Bronk, M. R. Mulholland, & E. J. Carpenter (Eds.), *Nitrogen in the Marine*
- 878 *Environment (Second Edition)* (pp. 529–567). Academic Press.

- 879 <https://doi.org/10.1016/B978-0-12-372522-6.00011-6>
- 880 Parker, A. E., Hogue, V. E., Wilkerson, F. P., & Dugdale, R. C. (2012). The effect of inorganic  
881 nitrogen speciation on primary production in the San Francisco Estuary. *Estuarine, Coastal  
882 and Shelf Science*, 104–105, 91–101. <https://doi.org/10.1016/j.ecss.2012.04.001>
- 883 Pennock, J. R., & Sharp, J. H. (1986). Phytoplankton production in the Delaware Estuary:  
884 Temporal and spatial variability. *Marine Ecology Progress Series*, 34(1/2), 143–155.
- 885 Pickett, S. T. A., Cadenasso, M. L., Grove, J. M., Boone, C. G., Groffman, P. M., Irwin, E.,  
886 Kaushal, S. S., Marshall, V., McGrath, B. P., Nilon, C. H., Pouyat, R. V., Szlavecz, K.,  
887 Troy, A., & Warren, P. (2011). Urban ecological systems: Scientific foundations and a  
888 decade of progress. *Journal of Environmental Management*, 92(3), 331–362.  
889 <https://doi.org/10.1016/j.jenvman.2010.08.022>
- 890 Pimm, S. L. (1984). The complexity and stability of ecosystems. *Nature*, 307(5949), 321–326.  
891 <https://doi.org/10.1038/307321a0>
- 892 Poff, N. L., Bledsoe, B. P., & Cuhaciyan, C. O. (2006). Hydrologic variation with land use across  
893 the contiguous United States: Geomorphic and ecological consequences for stream  
894 ecosystems. *Geomorphology*, 79(3), 264–285.  
895 <https://doi.org/10.1016/j.geomorph.2006.06.032>
- 896 QGIS Development Team. (2023). *QGIS Geographic Information System*.  
897 <https://www.qgis.org/en/site/>
- 898 Rabalais, N. N., Díaz, R. J., Levin, L. A., Turner, R. E., Gilbert, D., & Zhang, J. (2010). Dynamics  
899 and distribution of natural and human-caused hypoxia. *Biogeosciences*, 7(2), 585–619.  
900 <https://doi.org/10.5194/bg-7-585-2010>
- 901 Raimonet, M., & Cloern, J. E. (2017). Estuary–ocean connectivity: Fast physics, slow biology.

- 902           *Global Change Biology*, 23(6), 2345–2357. <https://doi.org/10.1111/gcb.13546>
- 903   Raymond, P. A., & Cole, J. J. (2001). Gas exchange in rivers and estuaries: Choosing a gas transfer  
904           velocity. *Estuaries*, 24(2), 312–317. <https://doi.org/10.2307/1352954>
- 905   Raymond, P. A., Zappa, C. J., Butman, D., Bott, T. L., Potter, J., Mulholland, P., Laursen, A. E.,  
906           McDowell, W. H., & Newbold, D. (2012). Scaling the gas transfer velocity and hydraulic  
907           geometry in streams and small rivers: Gas transfer velocity and hydraulic geometry.  
908           *Limnology and Oceanography: Fluids and Environments*, 2(1), 41–53.  
909           <https://doi.org/10.1215/21573689-1597669>
- 910   Redfield, A. C. (1934). On the Properties of Organic Derivatives in Sea Water and Their Relation  
911           to Composition of the Phytoplankton. In *James Johnstone Memorial Volume* (pp. 176–  
912           192). University Press of Liverpool.
- 913   Reisinger, A. J., Groffman, P. M., & Rosi-Marshall, E. J. (2016). Nitrogen-cycling process rates  
914           across urban ecosystems. *FEMS Microbiology Ecology*, 92(12), fiw198.  
915           <https://doi.org/10.1093/femsec/fiw198>
- 916   Reisinger, A. J., Rosi, E. J., Bechtold, H. A., Doody, T. R., Kaushal, S. S., & Groffman, P. M.  
917           (2017). Recovery and resilience of urban stream metabolism following Superstorm Sandy  
918           and other floods. *Ecosphere*, 8(4), e01776. <https://doi.org/10.1002/ecs2.1776>
- 919   Russell, S. J., Windham-Myers, L., Stuart-Haëntjens, E. J., Bergamaschi, B. A., Anderson, F.,  
920           Oikawa, P., & Knox, S. H. (2023). Increased salinity decreases annual gross primary  
921           productivity at a Northern California brackish tidal marsh. *Environmental Research*  
922           *Letters*, 18(3), 034045. <https://doi.org/10.1088/1748-9326/acbbdf>
- 923   Schimel, J. P., & Bennett, J. (2004). Nitrogen Mineralization: Challenges of a Changing Paradigm.  
924           *Ecology*, 85(3), 591–602. <https://doi.org/10.1890/03-8002>

- 925 Schindler, D. W. (1977). Evolution of Phosphorus Limitation in Lakes. *Science*, *195*(4275), 260–  
926 262. <https://doi.org/10.1126/science.195.4275.260>
- 927 Scully, M. E. (2010). Wind Modulation of Dissolved Oxygen in Chesapeake Bay. *Estuaries and*  
928 *Coasts*, *33*(5), 1164–1175. <https://doi.org/10.1007/s12237-010-9319-9>
- 929 Simon, A., & Rinaldi, M. (2006). Disturbance, stream incision, and channel evolution: The roles  
930 of excess transport capacity and boundary materials in controlling channel response.  
931 *Geomorphology*, *79*(3), 361–383. <https://doi.org/10.1016/j.geomorph.2006.06.037>
- 932 Smith, B. K., & Smith, J. A. (2015). The Flashiest Watersheds in the Contiguous United States.  
933 *Journal of Hydrometeorology*, *16*(6), 2365–2381. [https://doi.org/10.1175/JHM-D-14-](https://doi.org/10.1175/JHM-D-14-0217.1)  
934 [0217.1](https://doi.org/10.1175/JHM-D-14-0217.1)
- 935 Smith, S. V. (1984). Phosphorus versus nitrogen limitation in the marine environment. *Limnology*  
936 *and Oceanography*, *29*(6), 1149–1160. <https://doi.org/10.4319/lo.1984.29.6.1149>
- 937 Song, C., Dodds, W. K., Rüegg, J., Argerich, A., Baker, C. L., Bowden, W. B., Douglas, M. M.,  
938 Farrell, K. J., Flinn, M. B., Garcia, E. A., Helton, A. M., Harms, T. K., Jia, S., Jones, J. B.,  
939 Koenig, L. E., Kominoski, J. S., McDowell, W. H., McMaster, D., Parker, S. P., ...  
940 Ballantyne, F. (2018). Continental-scale decrease in net primary productivity in streams  
941 due to climate warming. *Nature Geoscience*, *11*(6), Article 6.  
942 <https://doi.org/10.1038/s41561-018-0125-5>
- 943 Sullivan, B. W., Alvarez-Clare, S., Castle, S. C., Porder, S., Reed, S. C., Schreeg, L., Townsend,  
944 A. R., & Cleveland, C. C. (2014). Assessing nutrient limitation in complex forested  
945 ecosystems: Alternatives to large-scale fertilization experiments. *Ecology*, *95*(3), 668–681.  
946 <https://doi.org/10.1890/13-0825.1>
- 947 Thayne, M. W., Kraemer, B. M., Mesman, J. P., Ibelings, B. W., & Adrian, R. (2022). Antecedent



- 948 lake conditions shape resistance and resilience of a shallow lake ecosystem following  
949 extreme wind storms. *Limnology and Oceanography*, 67(S1), S101–S120.  
950 <https://doi.org/10.1002/lno.11859>
- 951 Thayne, M. W., Kraemer, B. M., Mesman, J. P., Pierson, D., Laas, A., de Eyto, E., Ibelings, B.  
952 W., & Adrian, R. (2023). Lake surface water temperature and oxygen saturation resistance  
953 and resilience following extreme storms: Chlorophyll a shapes resistance to storms. *Inland  
954 Waters*, 13(3), 339–361. <https://doi.org/10.1080/20442041.2023.2242081>
- 955 Tsai, J.-W., Kratz, T. K., Hanson, P. C., Kimura, N., Liu, W.-C., Lin, F.-P., Chou, H.-M., Wu, J.-  
956 T., & Chiu, C.-Y. (2011). Metabolic changes and the resistance and resilience of a  
957 subtropical heterotrophic lake to typhoon disturbance. *Canadian Journal of Fisheries and  
958 Aquatic Sciences*, 68(5), 768–780. <https://doi.org/10.1139/f2011-024>
- 959 Uehlinger, U. (2000). Resistance and resilience of ecosystem metabolism in a flood-prone river  
960 system. *Freshwater Biology*, 45(3), 319–332. [https://doi.org/10.1111/j.1365-  
961 2427.2000.00620.x](https://doi.org/10.1111/j.1365-2427.2000.00620.x)
- 962 U.S. EPA. (1993a). *Method 350.1: Nitrogen, Ammonia (Calorimetric, Automated Phenate)*  
963 (Revision 2.0). [https://www.epa.gov/esam/epa-method-3501-determination-ammonia-  
964 nitrogen-semi-automated-colorimetry](https://www.epa.gov/esam/epa-method-3501-determination-ammonia-nitrogen-semi-automated-colorimetry)
- 965 U.S. EPA. (1993b). *Method 446.0: In Vitro Determination of Chlorophylls a, b, c1+c2 and  
966 Pheopigments in Marine and Freshwater Algae by Visible Spectrophotometry (1.2)*.
- 967 Utz, R. M., Hopkins, K. G., Beesley, L., Booth, D. B., Hawley, R. J., Baker, M. E., Freeman, M.  
968 C., & L. Jones, K. (2016). Ecological resistance in urban streams: The role of natural and  
969 legacy attributes. *Freshwater Science*, 35(1), 380–397. <https://doi.org/10.1086/684839>
- 970 Van Meerbeek, K., Jucker, T., & Svenning, J.-C. (2021). Unifying the concepts of stability and

- 971 resilience in ecology. *Journal of Ecology*, 109(9), 3114–3132.  
972 <https://doi.org/10.1111/1365-2745.13651>
- 973 Vietz, G. J., Walsh, C. J., & Fletcher, T. D. (2016). Urban hydrogeomorphology and the urban  
974 stream syndrome: Treating the symptoms and causes of geomorphic change. *Progress in*  
975 *Physical Geography: Earth and Environment*, 40(3), 480–492.  
976 <https://doi.org/10.1177/0309133315605048>
- 977 Vitousek, P. M., & Howarth, R. W. (1991). Nitrogen limitation on land and in the sea: How can it  
978 occur? *Biogeochemistry*, 13(2), 87–115. <https://doi.org/10.1007/BF00002772>
- 979 Walsh, C. J., Roy, A. H., Feminella, J. W., Cottingham, P. D., Groffman, P. M., & Morgan, R. P.  
980 (2005). The urban stream syndrome: Current knowledge and the search for a cure. *Journal*  
981 *of the North American Benthological Society*, 24(3), 706–723. [https://doi.org/10.1899/04-](https://doi.org/10.1899/04-028.1)  
982 028.1
- 983 Wetz, M. S., & Yoskowitz, D. W. (2013). An ‘extreme’ future for estuaries? Effects of extreme  
984 climatic events on estuarine water quality and ecology. *Marine Pollution Bulletin*, 69(1),  
985 7–18. <https://doi.org/10.1016/j.marpolbul.2013.01.020>
- 986 Woodland, R. J., Thomson, J. R., Mac Nally, R., Reich, P., Evrard, V., Wary, F. Y., Walker, J. P.,  
987 & Cook, P. L. M. (2015). Nitrogen loads explain primary productivity in estuaries at the  
988 ecosystem scale. *Limnology and Oceanography*, 60(5), 1751–1762.  
989 <https://doi.org/10.1002/lno.10136>
- 990 Zahn, E., Welty, C., Smith, J. A., Kemp, S. J., Baeck, M.-L., & Bou-Zeid, E. (2021). The  
991 Hydrological Urban Heat Island: Determinants of Acute and Chronic Heat Stress in Urban  
992 Streams. *JAWRA Journal of the American Water Resources Association*, 57(6), 941–955.  
993 <https://doi.org/10.1111/1752-1688.12963>

- 994 Zarnetske, J. P., Haggerty, R., Wondzell, S. M., Bokil, V. A., & González-Pinzón, R. (2012).  
995 Coupled transport and reaction kinetics control the nitrate source-sink function of  
996 hyporheic zones. *Water Resources Research*, 48(11).  
997 <https://doi.org/10.1029/2012WR011894>
- 998 Zhang, J., Gilbert, D., Gooday, A. J., Levin, L., Naqvi, S. W. A., Middelburg, J. J., Scranton, M.,  
999 Ekau, W., Peña, A., Dewitte, B., Oguz, T., Monteiro, P. M. S., Urban, E., Rabalais, N. N.,  
1000 Ittekkot, V., Kemp, W. M., Ulloa, O., Elmgren, R., Escobar-Briones, E., & Van der Plas,  
1001 A. K. (2010). Natural and human-induced hypoxia and consequences for coastal areas:  
1002 Synthesis and future development. *Biogeosciences*, 7(5), 1443–1467.  
1003 <https://doi.org/10.5194/bg-7-1443-2010>
- 1004 Zhang, M., Krom, M. D., Lin, J., Cheng, P., & Chen, N. (2022). Effects of a Storm on the  
1005 Transformation and Export of Phosphorus Through a Subtropical River-Turbid Estuary  
1006 Continuum Revealed by Continuous Observation. *Journal of Geophysical Research:*  
1007 *Biogeosciences*, 127(8), e2022JG006786. <https://doi.org/10.1029/2022JG006786>
- 1008 Zhang, Q., Fisher, T. R., Trentacoste, E. M., Buchanan, C., Gustafson, A. B., Karrh, R., Murphy,  
1009 R. R., Keisman, J., Wu, C., Tian, R., Testa, J. M., & Tango, P. J. (2021). Nutrient limitation  
1010 of phytoplankton in Chesapeake Bay: Development of an empirical approach for water-  
1011 quality management. *Water Research*, 188, 116407.  
1012 <https://doi.org/10.1016/j.watres.2020.116407>
- 1013 Zheng, Y., Huang, J., Feng, Y., Xue, H., Xie, X., Tian, H., Yao, Y., Luo, L., Guo, X., & Liu, Y.  
1014 (2024). The Effects of Seasonal Wind Regimes on the Evolution of Hypoxia in Chesapeake  
1015 Bay: Results from A Terrestrial-Estuarine-Ocean Biogeochemical Modeling System.  
1016 *Progress in Oceanography*, 103207. <https://doi.org/10.1016/j.pocean.2024.103207>

1017 Zhi, W., Feng, D., Tsai, W.-P., Sterle, G., Harpold, A., Shen, C., & Li, L. (2021). From  
1018 Hydrometeorology to River Water Quality: Can a Deep Learning Model Predict Dissolved  
1019 Oxygen at the Continental Scale? *Environmental Science & Technology*, 55(4), 2357–  
1020 2368. <https://doi.org/10.1021/acs.est.0c06783>

1021

1022 *Author Contribution Statement*

1023 E.B.G. and A.B.T. developed the study and interpreted the results. A.B.T. performed data analysis  
1024 and drafted the manuscript. All authors contributed to manuscript editing.

1025

1026 *Data Availability Statement:*

1027 This study used publicly available datasets, which included: 1) Long-term estuarine water quality,  
1028 nutrients and meteorological conditions and watershed boundaries for Lake Superior (LKS)  
1029 NERR, Chesapeake Bay, Maryland (CBM) NERR, Guana Tolomato Matanzas (GTM) NERR,  
1030 Weeks Bay (WKB) NERR, and San Francisco Bay (SFB) NERR stations from  
1031 <https://cdmo.baruch.sc.edu>; 2) Long-term precipitation data from U.S. airports from  
1032 <https://www.ncei.noaa.gov/cdo-web/datasets>; 3) Land use/land cover maps from  
1033 <https://livingatlas.arcgis.com/landcover/>; 4) U.S. population data from  
1034 <https://www.worldpop.org/>. Data and data processing code are also available at  
1035 <https://figshare.com/s/49d2f3dca084d885638a>.

1036

1037 **Supplementary Material for:**

1038

1039 **Title.** Physicochemical Factors and Urban Land-Use Characteristics Associated with Resistance  
1040 to Precipitation in Estuaries Vary Across Scales

1041

1042 **Authors and Affiliations**

1043 *Anna B. Turetcaia 0000-0003-1630-5741<sup>1,\*</sup>, anna.turetcaia@pnnl.gov*

1044 *Nicole G. Dix 0000-0002-0063-5167<sup>2</sup>, nikki.dix@dep.state.fl.us*

1045 *Hannah Ramage 0009-0004-2246-7696<sup>3</sup>, hannah.ramage@wisc.edu*

1046 *Matthew C. Ferner 0000-0002-4862-9663<sup>4</sup>, mferner@sfsu.edu*

1047 *and Emily B. Graham 0000-0002-4623-7076<sup>1,5,\*</sup>, emily.graham@pnnl.gov*

1048

1049 <sup>1</sup> Pacific Northwest National Laboratory, Richland, WA 99352, USA

1050 <sup>2</sup> Guana Tolomato Matanzas National Estuarine Research Reserve, Ponte Vedra Beach, FL 32082,  
1051 USA

1052 <sup>3</sup> Lake Superior National Estuarine Research Reserve, University of Wisconsin Madison, Division  
1053 of Extension, Superior, WI 54880, USA

1054 <sup>4</sup> San Francisco State University, Estuary and Ocean Science Center, Tiburon, CA 94920, USA

1055 <sup>5</sup> School of Biological Sciences, Washington State University, Pullman, WA 99164, USA

1056

1057

1058 **Supplementary Tables.**

1059

1060 **Table S1:** Multiparameter sonde position within the water column at five National Estuarine  
 1061 Research Reserve Systems (NERRS).

<b>Estuary</b>	<b>Monitoring location</b>	<b>Sonde position above sediment bed (m)</b>
Lake Superior (LKS)	Barker’s Island (BA)	0.5
	Pokegama Bay (PO)	0.25
	Blatnik Bridge (BL)	5.5
	Oliver Bridge (OL)	6.5
Chesapeake Bay, Maryland (CBM)	Iron Pot Landing (IP)	0.25
	Railroad Bridge (RR)	0.25
	Mataponi Creek (MC)	0.25
Weeks Bay (WKB)	Magnolia River (MR)	0.5
	Middle Bay (MB)	0.5
	Weeks Bay (WB)	0.5
	Fish River (FR)	0.5

Guana Tolomato-Matanzas (GTM)	San Sebastian (SS)	1.0
	Pine Island (PI)	1.0
	Pellicer Creek (PC)	1.0
	Fort Matanzas (FM)	1.0
San Francisco Bay (SFB)	First Mallard (FM)	0.25 - 0.5
	Second Mallard (SM)	0.25 - 0.5
	Gallinas Creek (GC)	0.25 - 0.5
	China Camp (CC)	0.25 - 0.5

1062

1063 **Table S2.** Datetime and threshold values for major precipitation events, and breakdown of the  
 1064 number of events during wet and dry years at each National Estuarine Research Reserve (NERR)  
 1065 station.

NERR Station	Datetime used to select dissolved oxygen and precipitation measurements to calculate the resistance index		Precipitation event (mm)	Wet/Dry year	Precipitation threshold (mm/day)
	Prior to disturbance (C <sub>0</sub> )	During and post disturbance (P <sub>0</sub> )			
Lake Superior, WI (LKS)	2017/06/24 00:00:00 -2017/06/27 23:45:00	2017/06/28 06:00:00 -2017/06/29 23:45:00	34.4	Wet (4)	> 25
	2017/07/30 00:00:00 -2017/08/02 23:45:00	2017/08/03 00:00:00 -2017/08/04 23:45:00	38.1		
	2017/08/23 00:00:00 -2017/08/25 23:45:00	2017/08/26 00:00:00 -2017/08/28 23:45:00	61.0		
	2017/09/29 00:00:00 -2017/10/01 23:45:00	2017/10/02 00:00:00 -2017/10/05 23:45:00	44.2		
	2020/07/14 00:00:00 -2020/07/17 23:45:00	2020/07/18 00:00:00 -2020/07/19 23:45:00	42.9	Dry (3)	
2020/07/14 00:00:00 -2020/07/17 23:45:00	2020/07/21 00:00:00 -2020/07/23 23:45:00	29.6			
2020/08/04 00:00:00 -2020/08/06 23:45:00	2020/08/07 12:00:00 -2020/08/11 23:45:00	74.9			

Chesapeake Bay, MD (CBM)	2018/05/10 00:00:00 -2018/05/11 12:00:00	2018/05/16 00:00:00 -2018/05/21 23:45:00	117.1	Wet (7)	>25	
	2018/05/24 00:00:00 -2018/05/26 23:45:00	2018/05/27 15:00:00 -2018/05/28 23:45:00	40.2			
	2018/05/24 00:00:00 -2018/05/26 23:45:00	2018/06/03 06:00:00 -2018/06/07 23:45:00	56.2			
	2018/06/16 00:00:00 -2018/06/18 23:45:00	2018/06/19 12:00:00 -2018/06/25 23:45:00	41.8			
	2018/07/13 00:00:00 -2018/07/16 23:45:00	2018/07/21 12:00:00 -2018/07/27 23:45:00	218.1			
	2018/09/04 00:00:00 -2018/09/06 23:45:00	2018/09/09 00:00:00 -2018/09/10 23:45:00	49.1			
	2018/09/13 00:00:00 -2018/09/15 23:45:00	2018/09/23 00:00:00 -2018/09/25 23:45:00	58.6			
	2016/06/24 00:00:00 -2016/06/27 23:45:00	2016/07/01 12:00:00 -2016/07/02 23:45:00	41.0	Dry (3)		
	2016/09/15 00:00:00 -2016/09/18 23:45:00	2016/09/19 00:00:00 -2016/09/19 23:45:00	25.2			
	2016/09/23 00:00:00 -2016/09/25 23:45:00	2016/09/28 00:00:00 -2016/09/30 23:45:00	76.4			
Guana Tolomato Matanzas, FL (GTM)	2017/08/19 00:00:00 -2017/08/22 23:45:00	2017/09/10 00:00:00 -2017/09/21 23:45:00	222.9	Wet (3)	*	
	2017/08/19 00:00:00 -2017/08/22 23:45:00	2017/09/30 00:00:00 -2017/10/13 23:45:00	270.7			
	2017/11/15 00:00:00 -2017/11/22 23:45:00	2017/11/23 00:00:00 -2017/11/25 23:45:00	123.1			
	2016/06/01 00:00:00 -2016/06/04 23:45:00	2016/06/05 12:00:00 -2016/06/07 23:45:00	127.9	Dry (4)		
	2016/08/21 00:00:00 -2016/08/27 23:45:00	2016/08/28 00:00:00 -2016/09/06 23:45:00	67.2			
	2016/09/05 00:00:00 -2016/09/08 23:45:00	2016/09/14 00:00:00 -2016/09/19 23:45:00	27.3			
	2016/09/21 00:00:00 -2016/09/25 23:45:00	2016/09/28 00:00:00 -2016/10/17 23:45:00	193.3			
Weeks Bay, AL (WKB)	2018/05/19 00:00:00 -2018/05/22 23:45:00	2018/05/23 00:00:00 -2018/05/27 23:45:00	90.9	Wet (8)	> 30	
	2018/06/07 00:00:00 -2018/06/09 23:45:00	2018/06/11 00:00:00 -2018/06/13 23:45:00	47.0			
	2018/06/28 00:00:00 -2018/06/30 23:45:00	2018/07/01 12:00:00 -2018/07/09 23:45:00	86.3			
	2018/07/12 00:00:00 -2018/07/14 23:45:00	2018/07/16 09:00:00 -2018/07/18 23:45:00	53.7			
	2018/08/25 00:00:00 -2018/08/26 23:45:00	2018/09/01 00:00:00 -2018/09/03 23:45:00	56.6			
	2018/08/25 00:00:00 -2018/08/26 23:45:00	2018/09/04 00:00:00 -2018/09/08 23:45:00	128.6			
	2018/09/19 00:00:00 -2018/09/20 23:45:00	2018/09/21 12:00:00 -2018/09/23 23:45:00	46.7			
	2018/09/19 00:00:00 -2018/09/20 23:45:00	2018/09/24 00:00:00 -2018/09/29 23:45:00	66.5			
	2019/04/01 00:00:00 -2019/04/03 23:45:00	2019/04/04 09:00:00 -2019/04/04 23:45:00	40.0	Dry (7)		
	2019/04/15 00:00:00 -2019/04/17 23:45:00	**2019/04/26 15:00:00 -2019/04/28 23:45:00	32.9			
	2019/06/01 00:00:00 -2019/06/04 23:45:00	2019/06/06 00:00:00 -2019/06/13 23:45:00	116.1			
	2019/06/20 00:00:00 -2019/06/25 23:45:00	2019/07/13 00:00:00 -2019/07/15 23:45:00	89.1			
	2019/08/07 00:00:00 -2019/08/10 23:45:00	2019/08/15 12:00:00 -2019/08/16 23:45:00	37.0			
	2019/08/22 00:00:00 -2019/08/24 23:45:00	2019/08/26 06:00:00 -2019/08/27 06:00:00	48.2			
	2019/10/21 00:00:00 -2019/10/24 23:45:00	2019/10/30 00:00:00 -2019/11/01 23:45:00	61.8			
San Francisco Bay, CA (SFB)	2017/01/01 00:00:00 -2017/01/02 06:00:00	2017/01/03 00:00:00 -2017/01/06 00:00:00	38.7		Wet (5)	> 20
	2017/01/01 00:00:00 -2017/01/02 06:00:00	2017/01/07 00:00:00 -2017/01/12 23:45:00	126.4			
	2017/01/01 00:00:00 -2017/01/02 06:00:00	2017/01/18 00:00:00 -2017/01/25 00:00:00	110.8			
	2017/03/11 00:00:00 -2017/03/17 23:45:00	2017/03/20 00:00:00 -2017/03/23 23:45:00	43.0			
	2017/04/01 00:00:00 -2017/04/05 06:00:00	2017/04/06 20:00:00 -2017/04/07 23:45:00	37.0			
	2018/01/06 00:00:00 -2018/01/07 23:45:00	2018/01/08 00:00:00 -2018/01/09 23:45:00	73.6	Dry (3)		
	2018/02/20 00:00:00 -2018/02/23 23:45:00	***2018/03/01 00:00:00 -2018/03/01 23:45:00	30.7			
	2018/04/04 12:00:00 -2018/04/05 12:00:00	2018/04/06 00:00:00 -2018/04/07 23:45:00	54.6			
<p>* For GTM 2016 the selected events were: Colin, Julia, Hermine, and Matthew. For 2017 the events were Irma and two Nor'easters.  ** This resistance calculation does not include dissolved oxygen measurements during the actual rain event from 2019/04/25 only dissolved oxygen after the event, because data during the event is missing from MB monitoring location.  *** Dissolved oxygen data for the SM site is missing. No resistance was calculated for SM during that time.</p>						

1066

1067

1068 **Table S3:** Pre-disturbance ( $C_0$ ) and post-disturbance ( $P_0$ ) dissolved oxygen ( $\text{mg L}^{-1}$ ) and the  
1069 resistance indices for each precipitation event across the estuaries. (.csv file)

1070



1071 **Table S4:** Resulting statistical parameters for linear regression analysis conducted for low- and  
 1072 high-salinity groups and on continental scale for five estuaries (this table accompanies Fig. 3).

Predictor variables regressed against mean resistance index values	Linear regression parameters:		
	Coefficient of determination ( $R^2$ )		
	Significance value ( $p$ )		
	Low salinity group	High-salinity group	Continental-scale
Turbidity (NTU)	$R^2 = 0.04$ $p = 0.327$	$R^2 = \mathbf{0.63}$ $p = \mathbf{0.001}$	$R^2 = 0.08$ $p = 0.097$
Salinity (ppt)	$R^2 = \mathbf{0.19}$ $p = \mathbf{0.029}$	$R^2 = 0.02$ $p = 0.66$	$R^2 = 0.001$ $p = 0.87$
Water temperature (C)	$R^2 = \mathbf{0.38}$ $p = \mathbf{0.001}$	$R^2 = \mathbf{0.6}$ $p = \mathbf{0.002}$	$R^2 = \mathbf{0.35}$ $p = \mathbf{0.0001}$
Water depth (m)	$R^2 = \mathbf{0.29}$ $p = \mathbf{0.006}$	$R^2 = 0.02$ $p = 0.635$	$R^2 = \mathbf{0.13}$ $p = \mathbf{0.027}$
$\log(\text{DIN})$ ( $\text{mg L}^{-1}$ )	$R^2 = 0.05$ $p = 0.268$	$R^2 = \mathbf{0.55}$ $p = \mathbf{0.004}$	$R^2 = \mathbf{0.12}$ $p = \mathbf{0.031}$
$\text{PO}_4^{-3}$ ( $\text{mg L}^{-1}$ )	$R^2 = 0.03$ $p = 0.416$	$R^2 = 0.06$ $p = 0.31$	$R^2 = 0.07$ $p = 0.134$

N:P	$R^2 = 0.14$ $p = 0.077$	<b><math>R^2 = 0.81</math></b> <b><math>p &lt; 0.0001</math></b>	$R^2 = 0.08$ $p = 0.101$
Chl- <i>a</i> ( $\mu\text{g L}^{-1}$ )	<b><math>R^2 = 0.46</math></b> <b><math>p = 0.0002</math></b>	<b><math>R^2 = 0.32</math></b> <b><math>p = 0.044</math></b>	<b><math>R^2 = 0.39</math></b> <b><math>p &lt; 0.0001</math></b>
Trees (%)	$R^2 = 0.01$ $p = 0.72$	<b><math>R^2 = 0.46</math></b> <b><math>p = 0.011</math></b>	$R^2 = 0.03$ $p = 0.30$
Crops (%)	$R^2 = 0.14$ $p = 0.07$	$R^2 = 0.05$ $p = 0.48$	$R^2 = 0.04$ $p = 0.22$
Built area (%)	$R^2 = 0.03$ $p = 0.41$	<b><math>R^2 = 0.73</math></b> <b><math>p = 0.0002</math></b>	<b><math>R^2 = 0.14</math></b> <b><math>p = 0.02</math></b>
Population density ( $\text{ppl km}^{-2}$ )	$R^2 = 0.16$ $p = 0.051$	<b><math>R^2 = 0.73</math></b> <b><math>p = 0.0002</math></b>	<b><math>R^2 = 0.27</math></b> <b><math>p = 0.001</math></b>

1073 Note: Significant correlations (i.e.,  $p < 0.05$ ) are shown in bold.

1074 **Supplementary figures.**

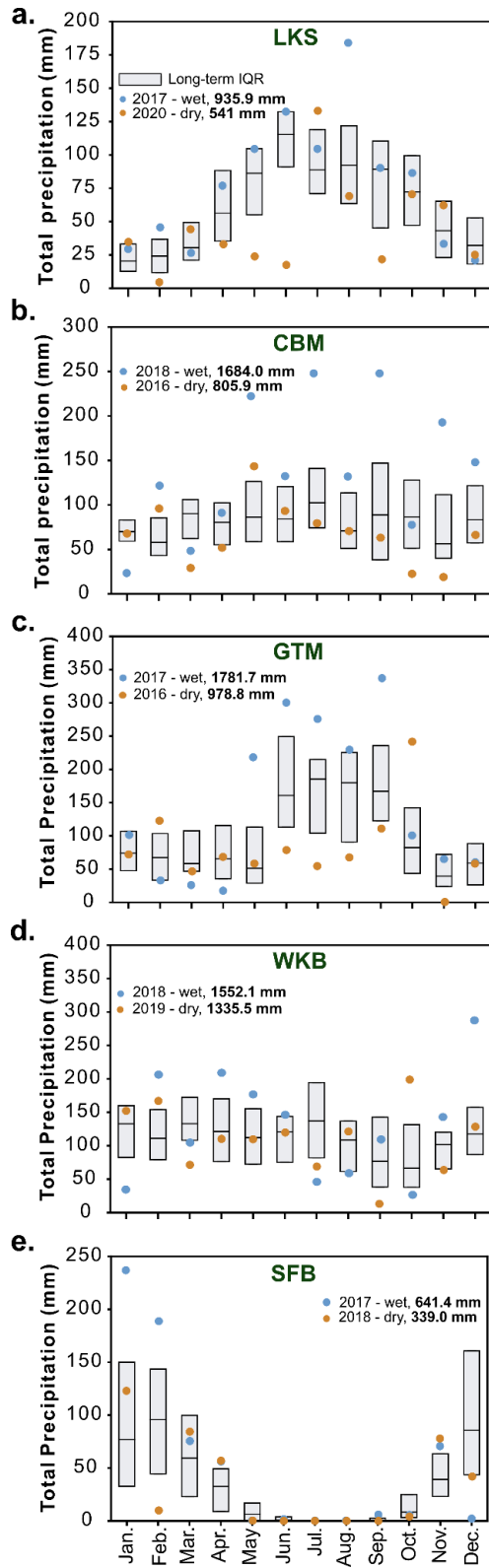
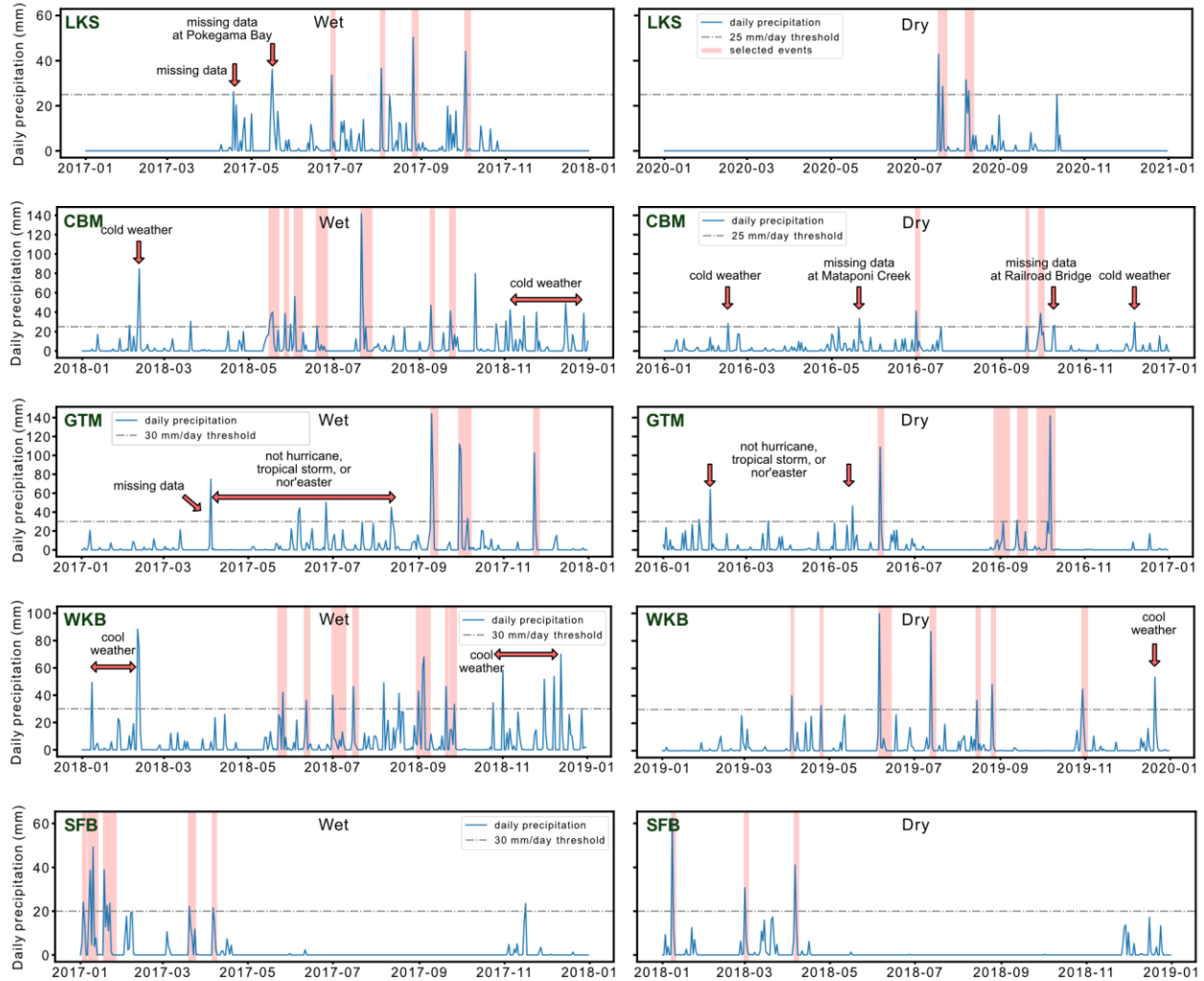


**Fig. S1.** Long-term (30-year) interquartile range and monthly precipitation during relatively wet and dry years. Long term precipitation data obtained from airports located in the vicinity of each selected estuarine station. a) Precipitation records from Duluth International airport were used to infer wet/dry years at Lake Superior (LKS) station. b) Washington Reagan International Airport precipitation records were used for Chesapeake Bay (CBM) station. c) Jacksonville International Airport precipitation record was used for Guana Tolomato Matanzas (GTM) station. d) Birmingham Airport precipitation records were used for Weeks Bay (WKS) station. e) San Francisco International Airport precipitation records were used for San Francisco Bay (SFB) station.

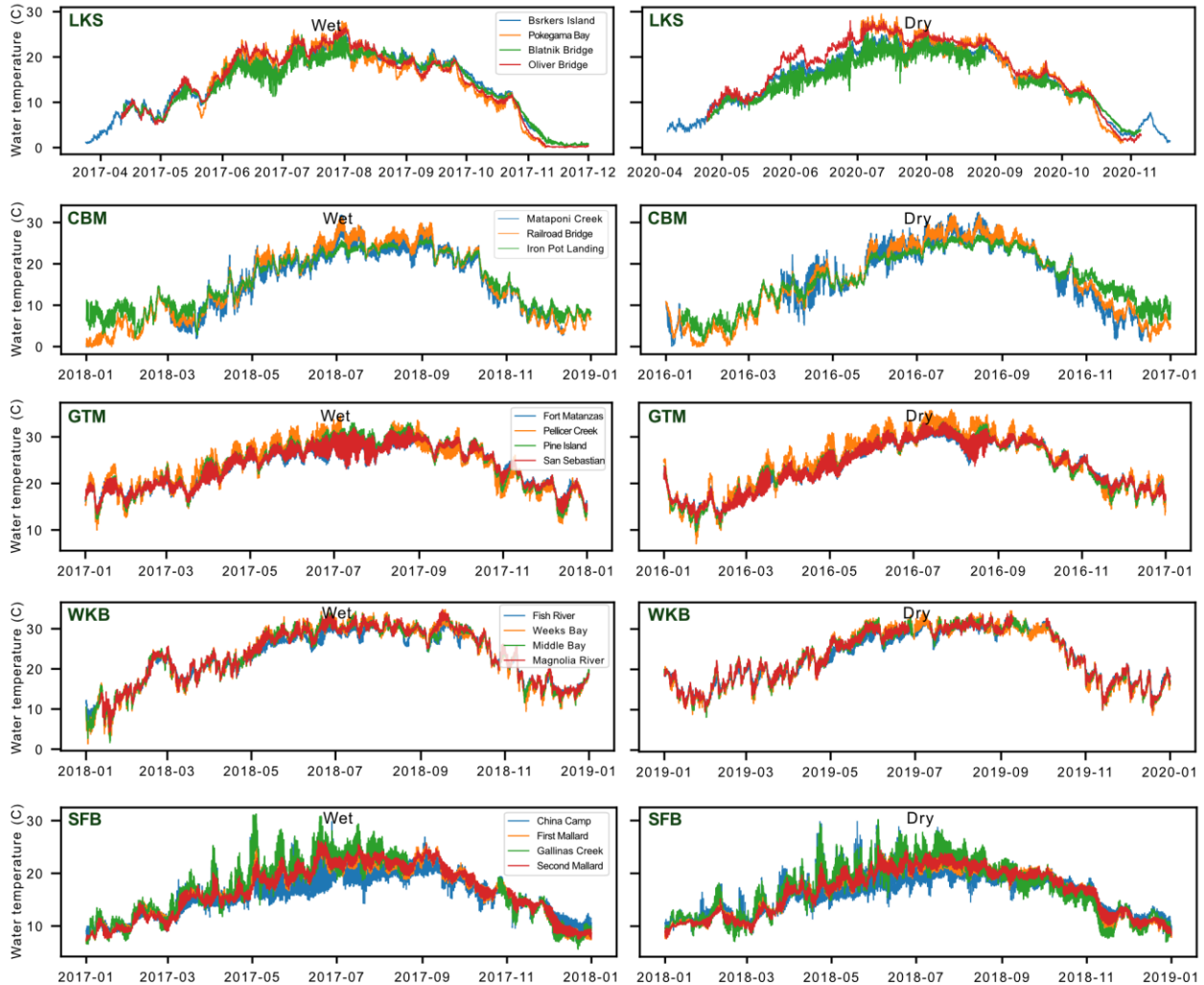
1075

1076



1077

1078 **Fig. S2.** Major precipitation events for each estuary during selected wet and dry years. The major  
 1079 precipitation events (shaded in red) identified by plotting National Estuarine Research Reserve  
 1080 (NERR) precipitation data collected at each estuary. The events were down selected based on water  
 1081 quality data availability for each estuary, within warmer seasons, and if the event was noted in  
 1082 NERR metadata sheets and/or reported as hurricane, tropical storm, or nor'easter. Estuary  
 1083 abbreviations: Lake Superior (LKS) NERR, Chesapeake Bay, Maryland (CBM) NERR, Guana  
 1084 Tolomato Matanzas (GTM) NERR, Weeks Bay (WKB) NERR, and San Francisco Bay (SFB)  
 1085 NERR. For details about events used for resistance index calculations, please see Table S2.



1086

1087 **Fig. S3.** Water temperature during selected wet and dry years for five National Estuarine Research

1088 Reserve (NERR) estuaries. Estuary abbreviations: Lake Superior (LKS) NERR, Chesapeake Bay,

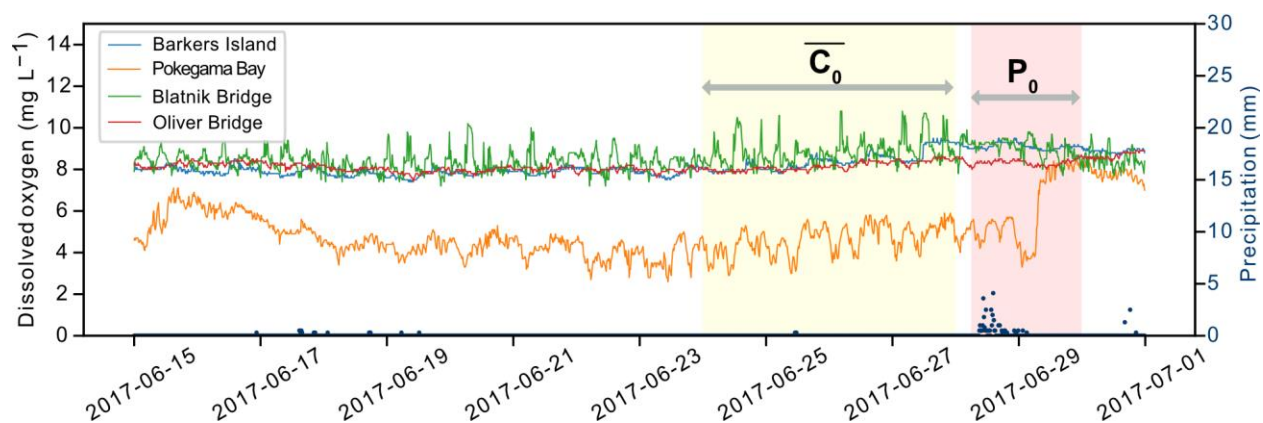
1089 Maryland (CBM) NERR, Guana Tolomato Matanzas (GTM) NERR, Weeks Bay (WKB) NERR,

1090 and San Francisco Bay (SFB) NERR. Note: At LKS, the water temperature record extends from

1091 April to December for 2017, and from April to November for 2020 because the St. Louis River

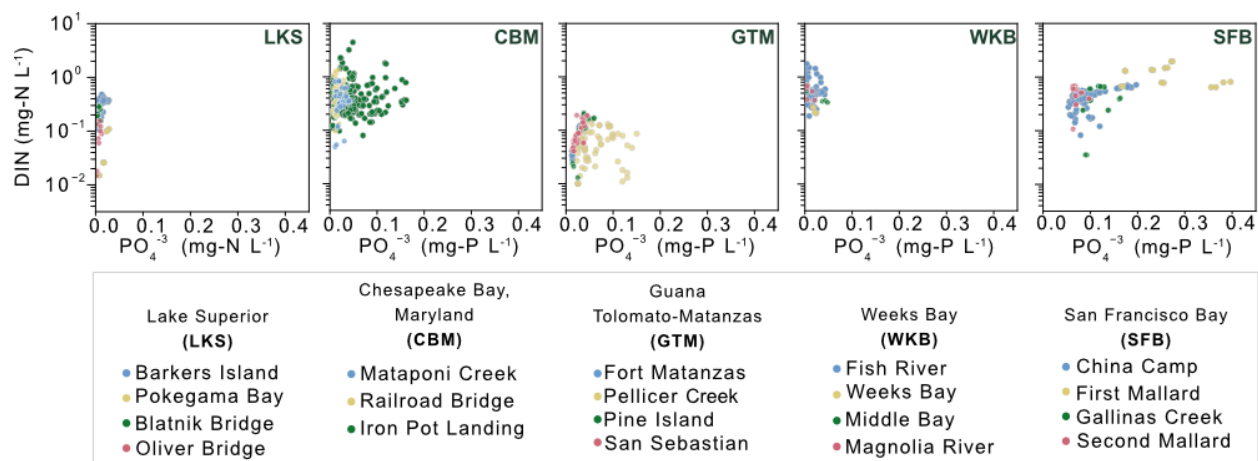
1092 freezes over and no measurements are collected.

1093



1094  
 1095 **Fig. S4.** Example for visualizing the selection of variables for resistance index calculations.  
 1096 Dissolved oxygen concentrations and precipitation at Lake Superior (LKS) NERR prior to and  
 1097 during a precipitation event on 06-28-2017. Yellow shaded box indicates the time used to calculate  
 1098 average pre-disturbance dissolved oxygen concentration (average  $C_0$ ). Red shaded box indicated  
 1099 the time used to identify dissolved oxygen concentration post-disturbance ( $P_0$ ).  $P_0$  was identified  
 1100 as the maximum displacement from average  $C_0$ .

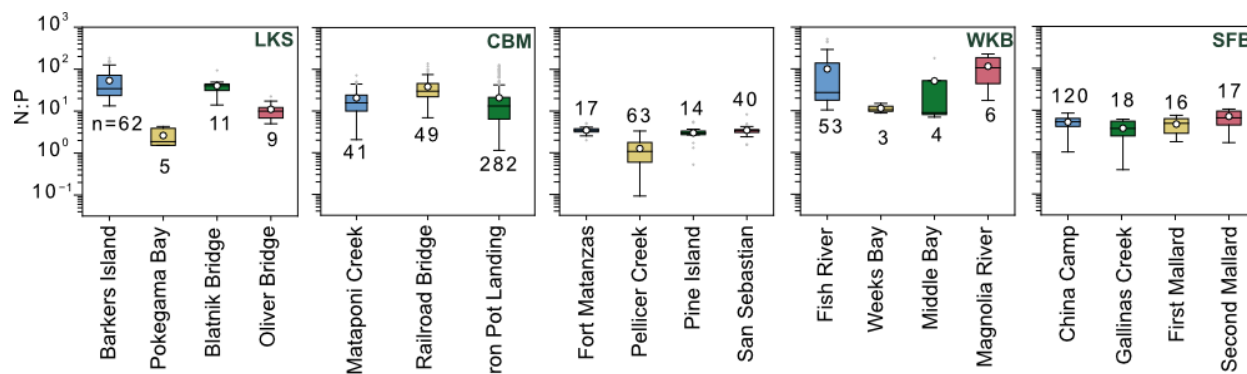
1101



1102

1103 **Fig. S5.** Dissolved inorganic nutrient concentrations at each estuary. Dissolved inorganic nitrogen  
 1104 (DIN) (i.e.,  $\text{NO}_3^- + \text{NO}_2^- + \text{NH}_4^+$ ). Estuary abbreviations: Lake Superior (LKS) NERR,  
 1105 Chesapeake Bay, Maryland (CBM) NERR, Guana Tolomato Matanzas (GTM) NERR, Weeks  
 1106 Bay (WKB) NERR, and San Francisco Bay (SFB) NERR. For LKS estuary, the  $\text{NH}_4^+$   
 1107 measurements for dry year (2020) were missing at all monitoring locations. For WKB, the  $\text{PO}_4^{3-}$   
 1108 measurements for wet-year (2018) were missing at WB, MB, and MR monitoring locations.

1109

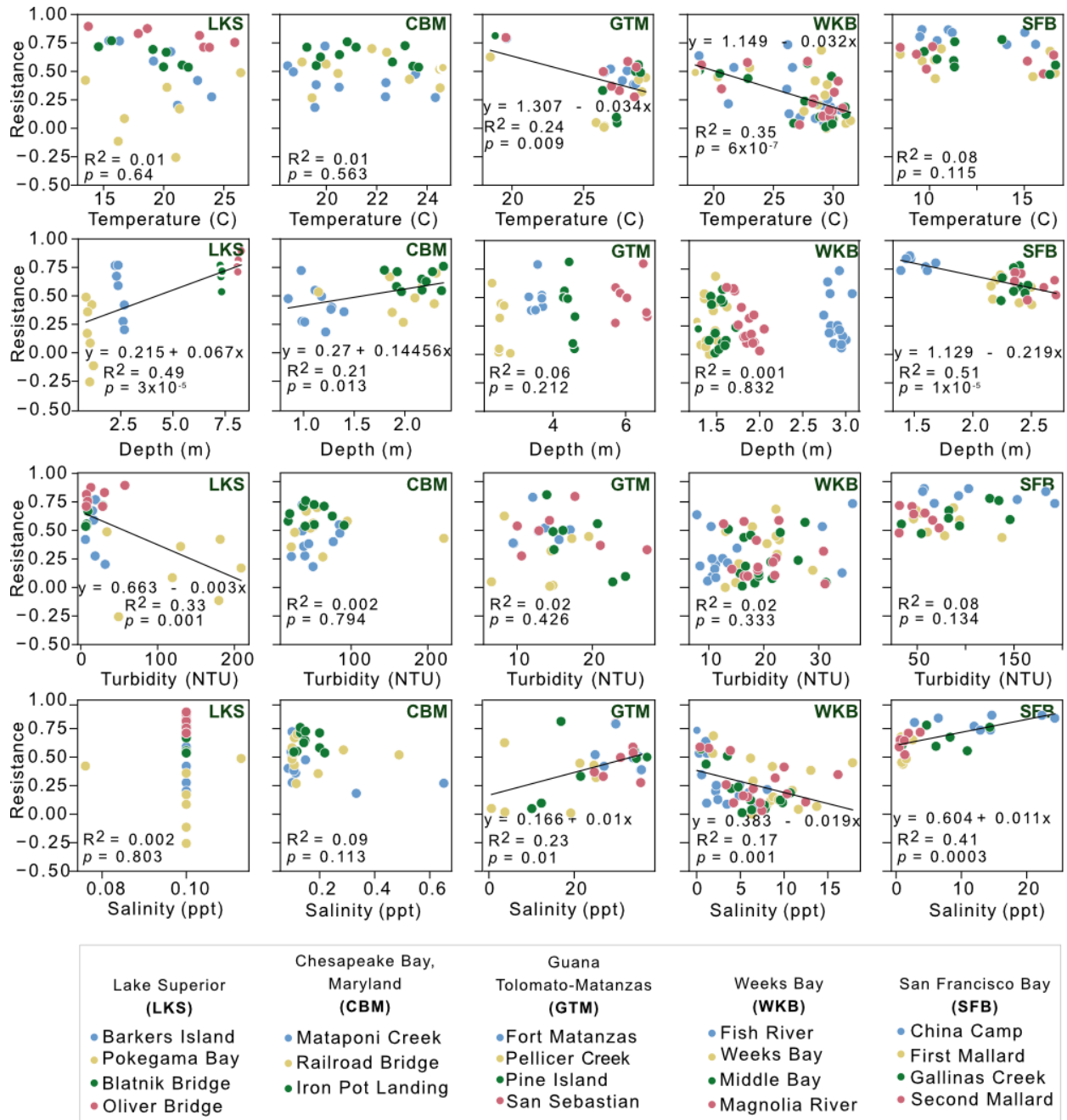


1110

1111 **Fig. S6.** Distribution of nitrogen to phosphorus ratio (N:P) within individual estuaries. Estuary  
 1112 abbreviations: Lake Superior (LKS) NERR, Chesapeake Bay, Maryland (CBM) NERR, Guana  
 1113 Tolomato Matanzas (GTM) NERR, Weeks Bay (WKB) NERR, and San Francisco Bay (SFB)  
 1114 NERR. Means are shown in white circles, and medians are shown in black solid lines. Boxes  
 1115 show the quartiles of the data set and the whiskers show the rest of the distribution. The  
 1116 stoichiometric N:P was calculated using dissolved inorganic nitrogen species (i.e.,  $\text{NO}_3^- + \text{NO}_2^-$   
 1117 +  $\text{NH}_4^+$ ) and phosphate. We note that because of missing measurements for  $\text{PO}_4^{3-}$  during the wet  
 1118 year at WKB- WB, MB, and MR – the N:P at these locations were calculated only for the dry  
 1119 year.



1120

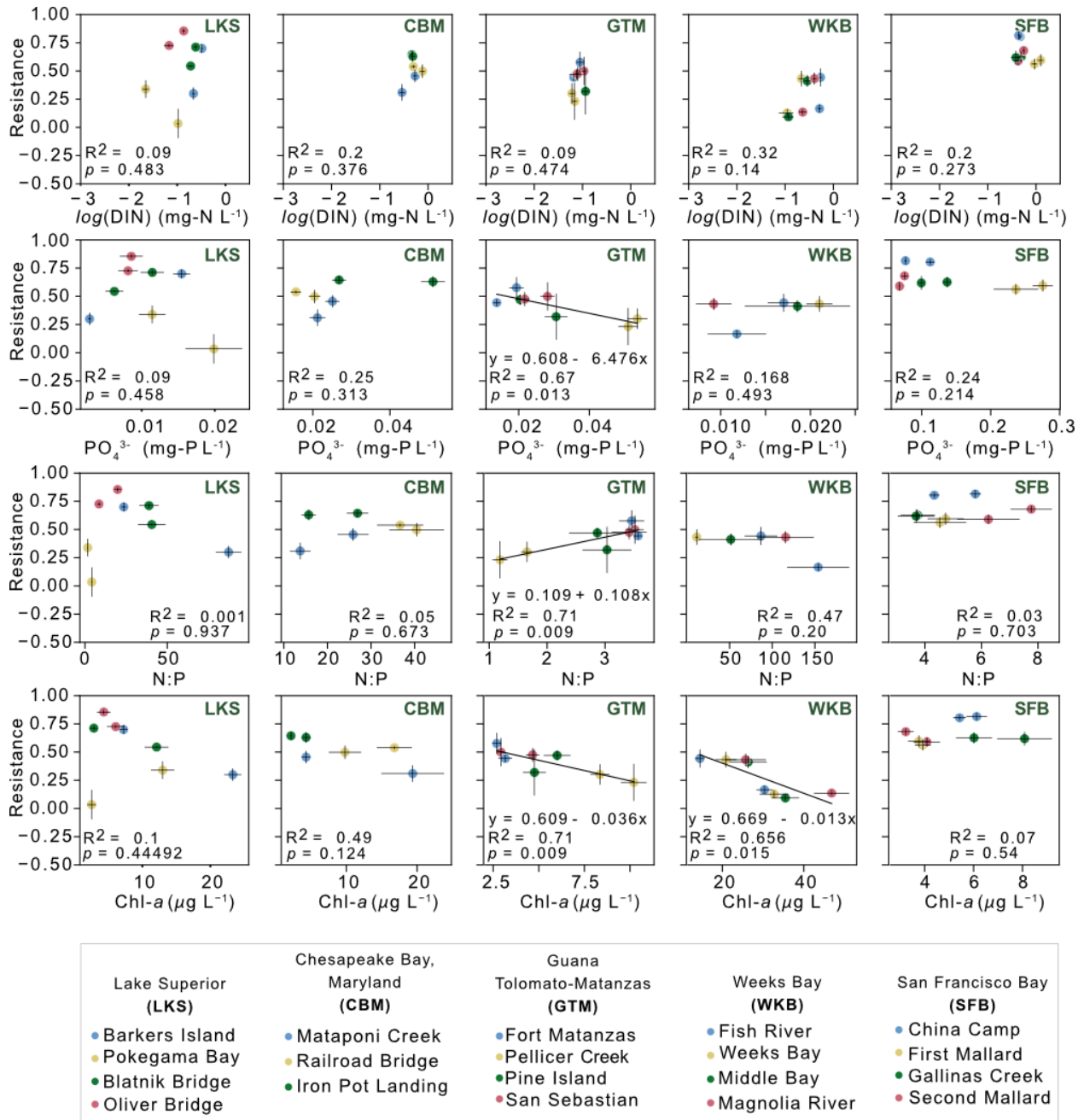


1121

1122 **Fig. S7.** Relationships of resistance to water temperature, water column depth, turbidity, and  
 1123 salinity at each estuary. Estuary abbreviations: Lake Superior (LKS) NERR, Chesapeake Bay,  
 1124 Maryland (CBM) NERR, Guana Tolomato Matanzas (GTM) NERR, Weeks Bay (WKB) NERR,  
 1125 and San Francisco Bay (SFB) NERR. Significant correlations ( $p < 0.05$ ) are shown in black lines.

1126 Relationships consider mean values of physicochemical factors in context of precipitation events  
1127 used in resistance index calculations (see dates in Table S2).  
1128

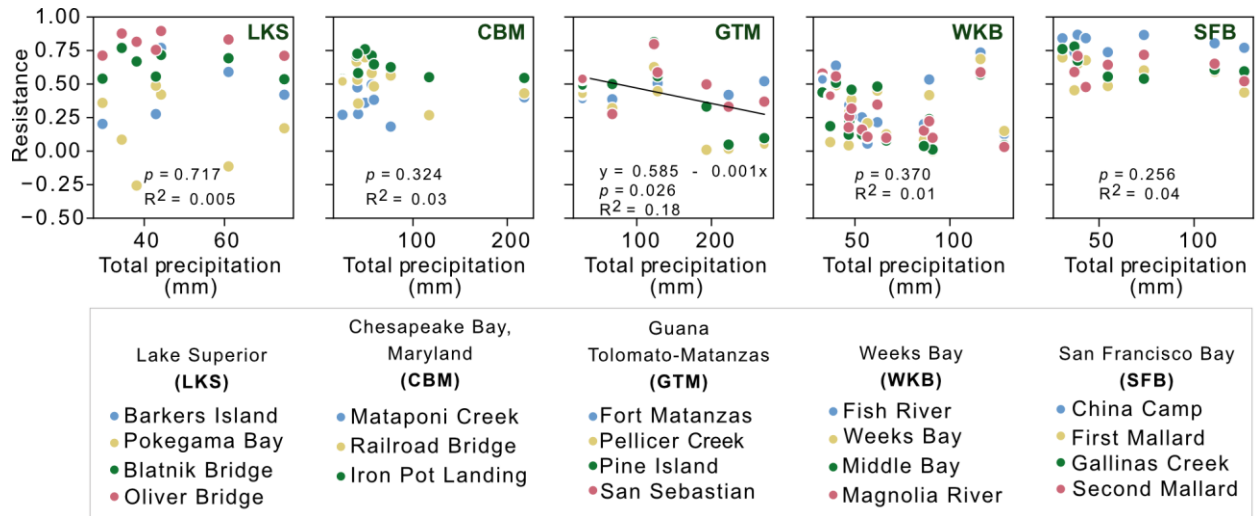
1129



1130

1131 **Fig. S8.** Relationships of resistance to dissolved inorganic nitrogen (DIN), phosphate (PO<sub>4</sub><sup>3-</sup>), N:P,  
 1132 and chlorophyll-a (Chl-a) at each estuary. Estuary abbreviations: Lake Superior (LKS) NERR,  
 1133 Chesapeake Bay, Maryland (CBM) NERR, Guana Tolomato Matanzas (GTM) NERR, Weeks Bay  
 1134 (WKB) NERR, and San Francisco Bay (SFB) NERR. Significant correlations ( $p < 0.05$ ) are shown

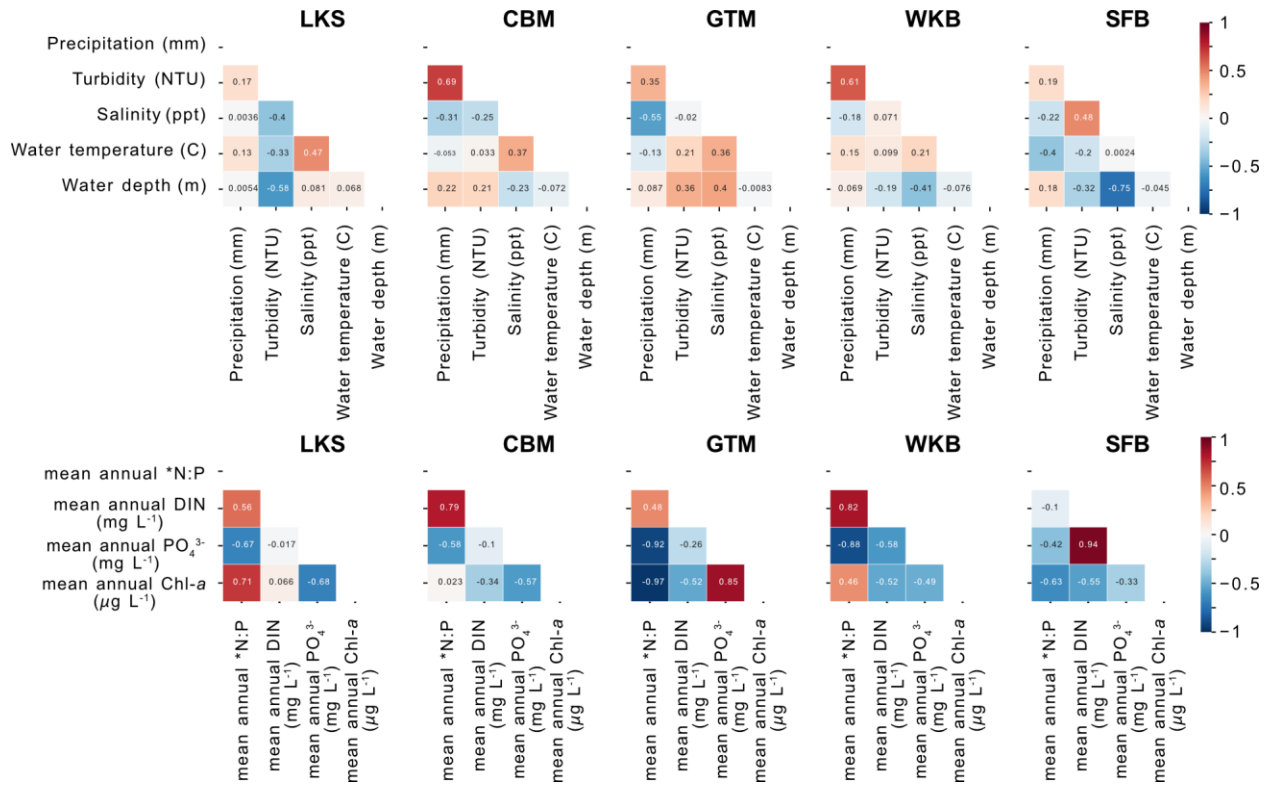
1135 in black. Standard errors of the mean are shown in horizontal and vertical black lines. Relationships  
1136 consider annual mean values of resistance and annual mean values for nutrients, N:P, and Chl-*a*  
1137 calculated for wet and dry years separately.



1138

1139 **Fig. S9.** Relationships between the resistance index and total precipitation during each event at  
 1140 each estuary. National Estuarine Reserve System (NERR) estuary abbreviations: Lake Superior  
 1141 (LKS) NERR, Chesapeake Bay, Maryland (CBM) NERR, Guana Tolomato Matanzas (GTM)  
 1142 NERR, Weeks Bay (WKB) NERR, and San Francisco Bay (SFB) NERR. Significant correlations  
 1143 ( $p < 0.05$ ) are indicated with a black line.

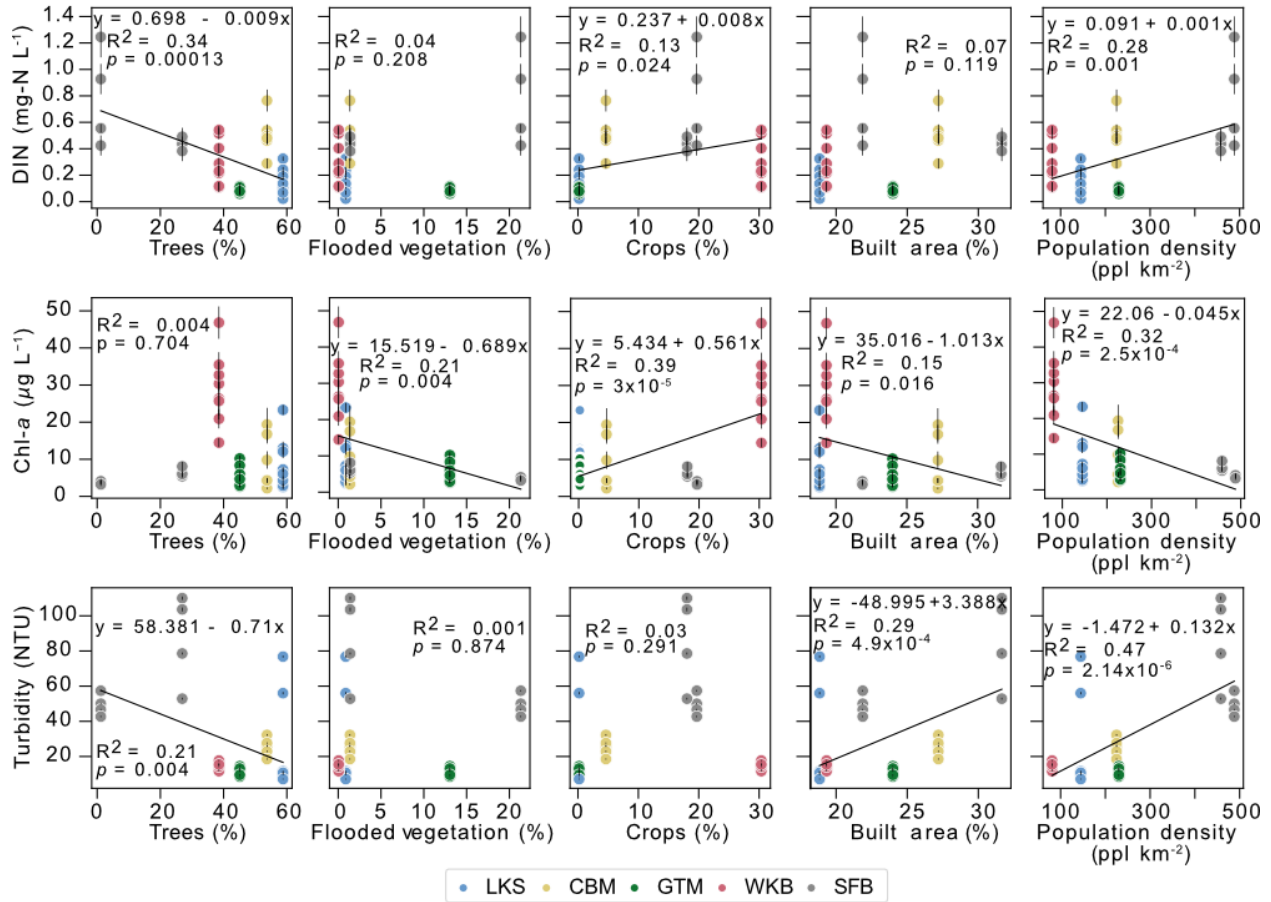
1144



1145

1146 **Fig. S10.** Correlation matrices for physicochemical parameters at each estuary.

1147



1148

1149 **Fig. S11.** Relationships of dissolved inorganic nitrogen (DIN), chlorophyll-*a* (Chl-*a*), and turbidity

1150 to land use/land cover and population density across estuaries. Estuary abbreviations: Lake

1151 Superior (LKS) NERR, Chesapeake Bay, Maryland (CBM) NERR, Guana Tolomato Matanzas

1152 (GTM) NERR, Weeks Bay (WKB) NERR, and San Francisco Bay (SFB) NERR. Regressions for

1153 significant relationships ( $p$ -value < 0.05) are shown in black lines. All relationships use annual

1154 means for physicochemical factors calculated for wet and dry years separately and land use/land

1155 cover characteristics adjoined to monitoring locations at each estuary.

1156